

**Doctoral Dissertation (Censored)**

**博士論文 (要約)**

**Development of Novel Heterogeneous Nickel Catalysts Utilizing  
Mesoporous Silica as a Support Material for Enantioselective  
1,4-Addition Reactions under Continuous-Flow Conditions**  
(連続フロー不斉 1,4-付加反応への適用を志向したメソポーラスシリカ担持新規不均一系ニッケル触媒の開発)

**A Dissertation Submitted for the Degree of Doctor of Philosophy**

令和元年 12月博士 (理学) 申請

**December 2019**

**Department of Chemistry, Graduate School of Science,**

**The University of Tokyo**

東京大学大学院理学系研究科

化学専攻

**Kan Kanai**

金井 歓

## Abstract

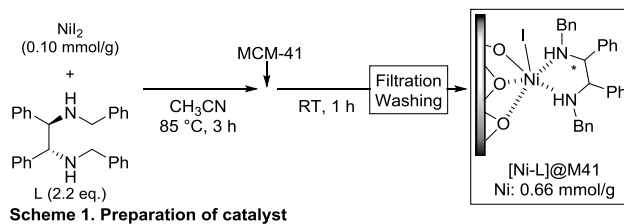
### *Development of Novel Heterogeneous Nickel Catalysts Utilizing Mesoporous Silica as a Support Material for Enantioselective 1,4-Addition Reactions under Continuous-Flow Conditions*

#### **Introduction**

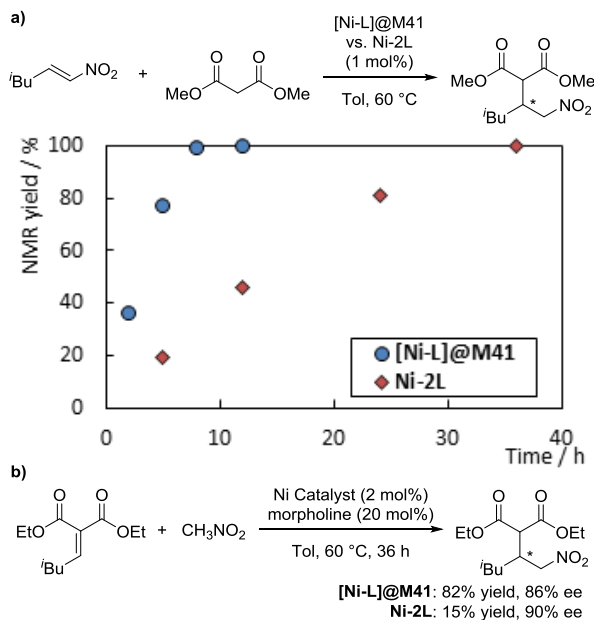
Although flow methods are very common in bulk chemical manufacturing, synthetic organic and process chemists have begun to pay much attention to the potential applications of flow methods for the synthesis of complex organic molecules since flow methods are safer to conduct, more efficient, and often generates less wastes compared to conventional batch methods.<sup>[a]</sup> In particular, continuous-flow reactions with columns packed with heterogeneous catalysts represents the ideal flow reactor since the immobilized catalysts can facilitate organic transformations under mild conditions and in a selective manner, and will remain in the reactors so that multiple columns can be connected together for multi-step flow reactions without the fear of downstream catalyst contamination. Although flow processes taking advantage of heterogeneous catalysis is in high demand, relative narrow sets of highly active and selective heterogeneous catalyst are available for flow synthesis. For instance, enantioselective heterogeneous catalysis under continuous-flow condition is important since many specialty chemicals, such as drugs, are chiral. However, relatively limited number of chiral heterogeneous catalysts have been examined for fine flow synthesis.<sup>[a]</sup> The most common approach of preparing chiral heterogeneous catalysts is through the attachment of catalytically active species on heterogeneous supports by utilizing a linker or spacer to mitigate undesirable influences from the support to the catalyst. However, these immobilized chiral catalysts are often inferior to their homogeneous counterparts, with respect to its reactivity and selectivity, and their preparation is often long and tedious. An alternative strategy for the immobilization of a chiral catalyst to a solid support is to utilize non-covalent bonding interactions, such as electrostatic or physiochemical absorption. Under flow conditions, a mobile phase including reactants penetrate into a static catalyst phase of a reactor along with close contact; thus, direct interaction between reactants with a catalyst phase through adsorption/desorption should be important. From these points of view, immobilization of chiral active sites directly onto supports by non-covalent bonding interactions is much suitable under flow conditions. However, a major challenge with this preparation method is the instability of these heterogeneous catalysts since non-covalent bonding is weaker than covalent bonding. It was hypothesized that mesoporous silica may represent an ideal support material for non-covalent immobilization of chiral metal complexes since the wide and uniform surface area and large pore space of these materials may provide a suitable environment that can efficiently immobilize the catalyst without diminishing its activity and selectivity. In this Ph.D. thesis, the utilization of chiral heterogeneous catalysts, generated through the impregnation of chiral metal complexes to mesoporous silica surface, for enantioselective reactions was examined.

## 1. Chiral nickel diamine complexes immobilized on mesoporous silica for asymmetric 1,4-addition reactions

In my master course study, the sequential-flow synthesis of racemic pregabalin, one of the world's top-selling drugs used for the treatment of various ailments, such as epilepsy, neuropathic pain, anxiety disorder, etc., was achieved.<sup>[b]</sup> Since the actual drug is a chiral compound, I decided to establish an



enantioselective flow synthesis of pregabalin with a chiral heterogeneous catalyst. For its synthesis, asymmetric 1,4-addition of a malonate to a nitroalkene is required to introduce chirality, and it was reported by Evans that a chiral nickel diamine complex was an effective catalysts for this organic transformation.<sup>[c]</sup> I hypothesized that impregnation of the chiral nickel diamine catalyst to a mesoporous silica support would lead to an efficient chiral heterogeneous catalyst. I found that a chiral complex prepared from nickel iodide and chiral diamine could be immobilized on mesoporous silica, MCM-41 (Scheme 1). I demonstrated that this chiral composite worked well as a heterogeneous catalyst for 1,4-addition reactions of dimethyl malonate with nitroalkenes. To understand the nature of the obtained heterogeneous catalyst, several experiments were performed. The nitrogen adsorption experiment indicated that the Brunauer-Emmett-Teller (BET) surface area and pore volume of the nickel-embedded sample decreased as the amount of nickel loaded on the support increased, while the external surface area was almost constant. This suggested that chiral nickel complexes were located inside of the MCM-41 mesopores. Quantitation of nickel and iodine in the solid catalyst and amount of the chiral ligand recovered during the heterogeneous catalyst preparation revealed that the proportion of the newly formed nickel species was in the ratio of 1:1:1 for nickel, iodine, and ligand, respectively. This was supported by Ni K-edge EXAFS studies, and while the 1:1 complex is known to be unstable under homogeneous conditions, I hypothesized that the formation of nickel silicate bond may be key in stabilizing this nickel complex. I also found that the prepared heterogeneous catalyst showed better activity than the homogeneous chiral nickel complex when dimethyl malonate was used a substrate (Scheme 2a). On the other hand, the reaction rate was reversed when the larger dibenzyl malonate was employed as the nucleophile, and these results also supported my assertion that the chiral nickel diamine complex is located within the mesopores of the silica support. In addition, I found that the same catalyst provided the first successful examples of enantioselective 1,4-addition of nitromethane to alkylidene malonates with the assistance of a catalytic amount of morpholine (Scheme 2b). Although organic bases can decompose the homogeneous chiral Ni-diamine complex through ligand exchange, the supported Ni-diamine was compatible with the base, presumably due to the stabilizing effect of the support to the chiral metal complex.



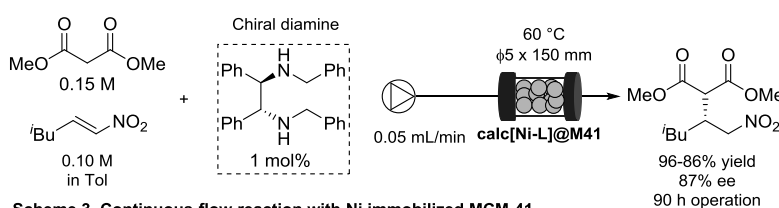
I also applied the chiral mesoporous material as a catalyst for asymmetric continuous-flow synthesis. The [Ni-L]@M-41 powder could be easily packed in a stainless column reactor, and was used for the enantioselective 1,4-addition in flow. The desired product was obtained in a good yield and enantioselectivity. Although the catalyst lifetime was somewhat limited, I found that by co-feeding the chiral diamine (0.2 mol%) with the substrates enable

the heterogeneous catalyst to be active for at least 1 day. Additionally, I demonstrated a two-step sequential-flow synthesis of (*S*)-pregabalin precursor by connecting the enantioselective addition reaction with a heterogeneous Pd-catalyzed hydrogenation reaction, and the desired  $\gamma$ -lactam was obtained in 89% yield with 87% ee.

## 2. Development of a robust nickel immobilized mesoporous silica for an asymmetric 1,4-addition reaction

In the previous section, I found that a new catalytic species was formed by treating a chiral Ni complex with mesoporous silica. However, single-site immobilization of the nickel species through I-Ni-O-Si bond led to a heterogeneous catalyst with a relatively poor lifetime that was incompatible for long-term operation in flow. In this study, I tested another approach to generate a more robust heterogeneous nickel catalyst through calcination. I used a surface modification technique with an achiral nickel diamine complex and MCM-41, and the obtained material was calcined at 450 °C in air to generate the desired nickel silicate bond and remove the achiral ligand. Asymmetric 1,4-addition of malonate to nitroalkene was used to evaluate the catalyst activity with external addition of a chiral diamine ligand. The continuous-flow reaction with the optimal calc[Ni-L]@M-41 and co-feeding 1 mol% chiral diamine ligand afforded the desired

product in 86% yield with 87% ee for 90 h operation (Scheme 3). Compared with the typical impregnation method or template ion-exchange method, the present surface modification method provided a more robust catalyst.



Scheme 3. Continuous-flow reaction with Ni immobilized MCM-41

## Conclusion

In my Ph. D. studies, I developed various heterogeneous catalysts for enantioselective addition reactions by taking advantage of the features of mesoporous silica. In the first topic, a chiral Ni-diamine complex was directly immobilized on the mesoporous silica, and this led to a heterogeneous catalyst that possessed superior catalyst activity and stability compared to the homogeneous catalyst for asymmetric 1,4-addition reactions of malonates to nitroalkenes and nitromethane to alkylidene malonates. In the second topic, a more robust heterogeneous nickel material was prepared by calcination, and this solid catalyst, in conjugation with a chiral diamine ligand, was utilized for a continuous-flow asymmetric 1,4-addition reaction that could be operated for 90 hours without significant deactivation of the catalyst.

## References

- [a] Kobayashi, S. *Chem. Asian. J.* **2016**, *11*, 425.
- [b] Ishitani, H.; Kanai, K.; Saito, Y.; Tsubogo, T.; Kobayashi, S. *Eur. J. Org. Chem.*, **2017**, 2017, 6491.
- [c] Evans, D. A.; Mito, S.; Seidel, D. *J. Am. Chem. Soc.* **2007**, *129*, 11583.

## **Acknowledgement**

First of all, I would like to express the deepest appreciation to Prof. Shū Kobayashi for his valuable suggestions, enthusiastic discussions, and continuous encouragement.

I really thank Dr. Haruro Ishitani for his support. He gave me many suggestions about research and presentation and had discussions with me a lot. Without his support, I could not progress in my Ph. D. study.

I also thank Prof. Tomoko Yoshida at Osaka City University for performing XAFS analysis of my catalysts.

I deeply thank Dr. Yasuhiro Yamashita, Dr. Hiroyuki Miyamura, Dr. Woo-Jin Yoo, Dr. Tomohiro Yasukawa, Dr. Taku Kitanosono, Dr. Min Hyemin, and Dr. Yuki Saito for beneficial advice and discussions.

I would like to express my appreciation to all continuous-flow members for every discussion and kind support for laboratory life. Thanks to flow members, I really enjoyed laboratory life.

I would also like to express my thanks to all Kobayashi Lab. members for a lot of help and discussions.

Finally, I would like to offer my special thanks to my family and friends for kind supports.

2020

Kan Kanai

## Table of Contents

### *Development of Novel Heterogeneous Nickel Catalysts Utilizing Mesoporous Silica as a Support Material for Enantioselective 1,4-Addition Reactions under Continuous-Flow Conditions*

<b>Abstract</b> .....	i
<b>Acknowledgement</b> .....	iv
<b>Table of Contents</b> .....	v
<b>Chapter 1. Introduction and Strategy</b> .....	1
1-1 Continuous-flow Reactions for Organic Synthesis .....	1
1-2 Classification of Continuous-flow Reactions. ....	2
1-3 Continuous-flow Reactions with Heterogeneous Catalysts.....	5
1-4 Heterogeneous Catalysts for Enantioselective Reactions.....	7
1-5 Design of Heterogeneous Catalysts for Continuous-flow Reactions .....	12
1-6 References.....	13
<b>Chapter 2. Chiral Nickel Diamine Complexes Immobilized on Mesoporous Silica for Asymmetric 1,4-Addition Reactions</b> .....	15
2-1 Background and Strategy.....	15
2-2 Catalyst Preparation and Characterization .....	18
2-3 Evaluation of Catalysts with 1,4-Addition of Malonate to Nitroalkene .....	24
2-4 Investigation of 1,4-Addition of Nitromethane to Alkylidene Malonate .....	30
2-5 Proposed Mechanism of 1,4-addition Reactions .....	35
2-6 Utilization of Catalysts for Continuous-flow Reactions .....	36
2-7 Demonstration of 2-Step Sequential-flow Synthesis of Pregabalin .....	39
2-8 Summary .....	42
2-9 References.....	43
<b>Chapter 3. Development of Robust Nickel Immobilized Mesoporous Silica for Asymmetric 1,4-Addition Reactions</b> .....	44
3-1 Background.....	44
3-2 Catalyst Preparation and Characterization .....	46
3-3 Evaluation of Catalyst Activity for Continuous-flow Reactions .....	51
3-4 Optimization of Conditions of Continuous-flow Reactions .....	55
3-5 Long Time Operations of Continuous-flow Reactions under Optimal Condition .....	58
3-6 Substrate Scope of 1,4-Addition Reactions under Continuous-flow Conditions .....	60
3-7 Summary .....	61
3-8 References .....	62
<b>Summary</b> .....	63
<b>Experimental Section in Chapter 2</b> .....	65
<b>Experimental Section in Chapter 3</b> .....	75

## Chapter 1. Introduction and Strategy

### 1-1 Continuous-flow reactions for organic synthesis

Chemical product manufacturing is performed in either of two methods: batch or flow method. Both methods are well known and have been developed since long time ago. In the field of mass production of basic chemicals, flow methods are more familiar than batch methods due to high efficiency. On the other hand, organic synthesis, which is employed in fine chemical production such as pharmaceuticals, perfumes, and agricultural chemicals etc., has been developed based on batch methods. In general batch reactions for organic synthesis, there are three operations, which are injection of starting materials into reactors, quenching reactions, and purification of desired products. One batch reaction costs much labor and solvent through these operations. In addition, when organic molecules having complex structure such as fine chemicals are synthesized by batch methods, several reactions must be combined for several chemical transformations, and it requires much amount of waste and manpower.

In recent years, continuous-flow reactions for organic synthesis have been well developed.<sup>1-5</sup> In flow reactions, starting materials are continuously injected into column reactors or tube reactors, and products are eluted incessantly. When a flow reaction connects to another flow reaction, several transformations could be performed in one operation. Considering this fact, flow reactions are superior to batch reactions in terms of environmental compatibility, efficiency, and safety.<sup>6-7</sup> In addition, specific advantages of flow reactions have been revealed by Yoshida group and Ley group. The former has developed micro flow reactions, which are able to utilize unstable intermediates by controlling reaction time in milliseconds using micro flow reactors.<sup>8</sup> The latter group has reported continuous-flow synthesis of natural products utilizing some of equipments and techniques.<sup>2</sup> Nevertheless, continuous-flow reactions for organic synthesis are still a developing field at a research and industrial level. Therefore, further expansion of fundamental research in continuous-flow chemistry is absolutely necessary to realize the conversion from a conventional batch process to an efficient continuous-flow process in organic synthesis.

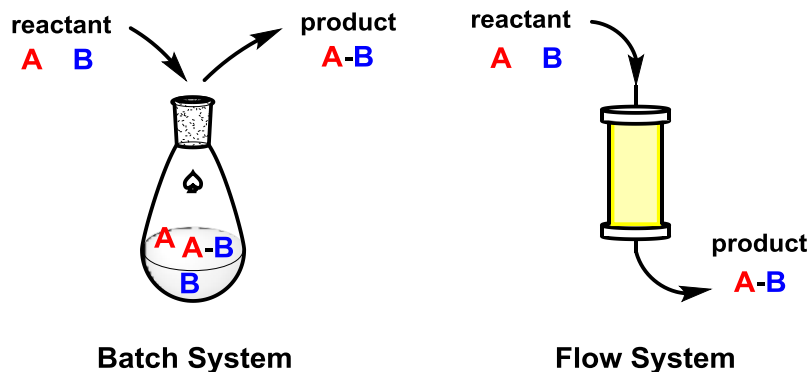


Figure 1-1-1. Type of chemical reactions

## 1-2 Classification of continuous-flow reactions

So far, various kinds of continuous-flow reactions have been reported, and they are classified into four types according to reaction types (Figure 1-2-1).<sup>5,9</sup> Type I is a spontaneous reaction, which proceeds while substrates go through a reactor. Micro flow reactions utilizing unstable active reagents correspond to type I reactions. Type II reactions are spontaneous reactions employing supported reagents. One reagent is injected into a reactor embedded another reagent, and a reaction proceeds to afford a product. In this manner, though selectivity of a reaction is controllable, replacement of a reactor is required at the time of complete consumption of the supported reagent. In modern organic chemistry, catalytic reactions are desirable from the viewpoint of green chemistry, and types III and IV reactions utilize homogeneous and heterogeneous catalysts, respectively. A homogeneous catalyst is flowed with substrates and catalyzes the reaction during passing through the reactor in type III reactions. Consequently, a mixture of product and a homogeneous catalyst is obtained from the end of the reactor. Further operation is needed to separate the homogeneous catalyst from the product. In type IV reactions, heterogeneous catalysts are packed in reactors, and substrates are injected into the reactors. The reaction undergoes through the reactor to give a product permanently as long as the catalyst activity is kept. As separation of a catalyst from a product is not required, the flow reaction can be directly connected to another flow reaction.

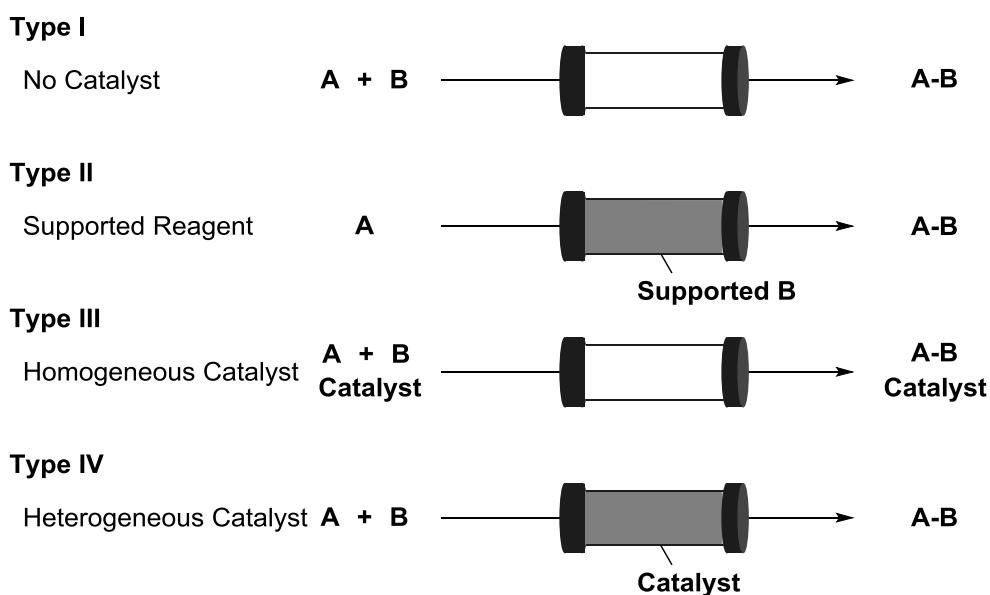
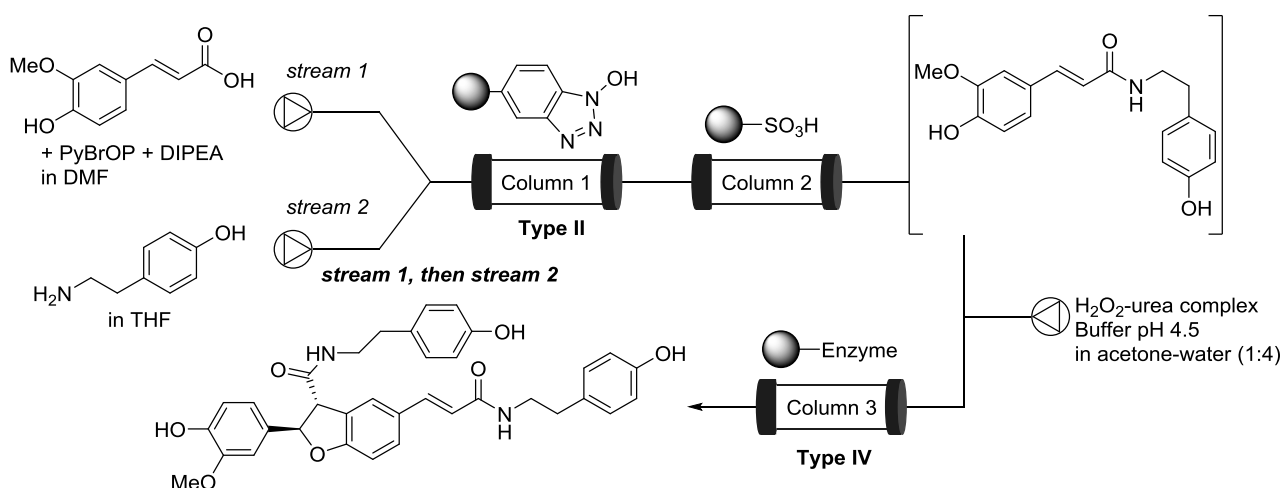


Figure 1-2-1. Classification of continuous-flow reactions

In general, continuous-flow synthesis of complex organic molecule is established by combining several types flow reactions. The first report of multistep continuous-flow synthesis of a natural product was grossamide synthesis described by S.V. Ley and co-workers (Scheme 1-2-1).<sup>10</sup> In this report, firstly, ferulic acid (stream 1) was introduced to the first column (Column 1), which was packed with polymer-supported hydroxybenzotriazole to immobilize activated ester in the Column 1.

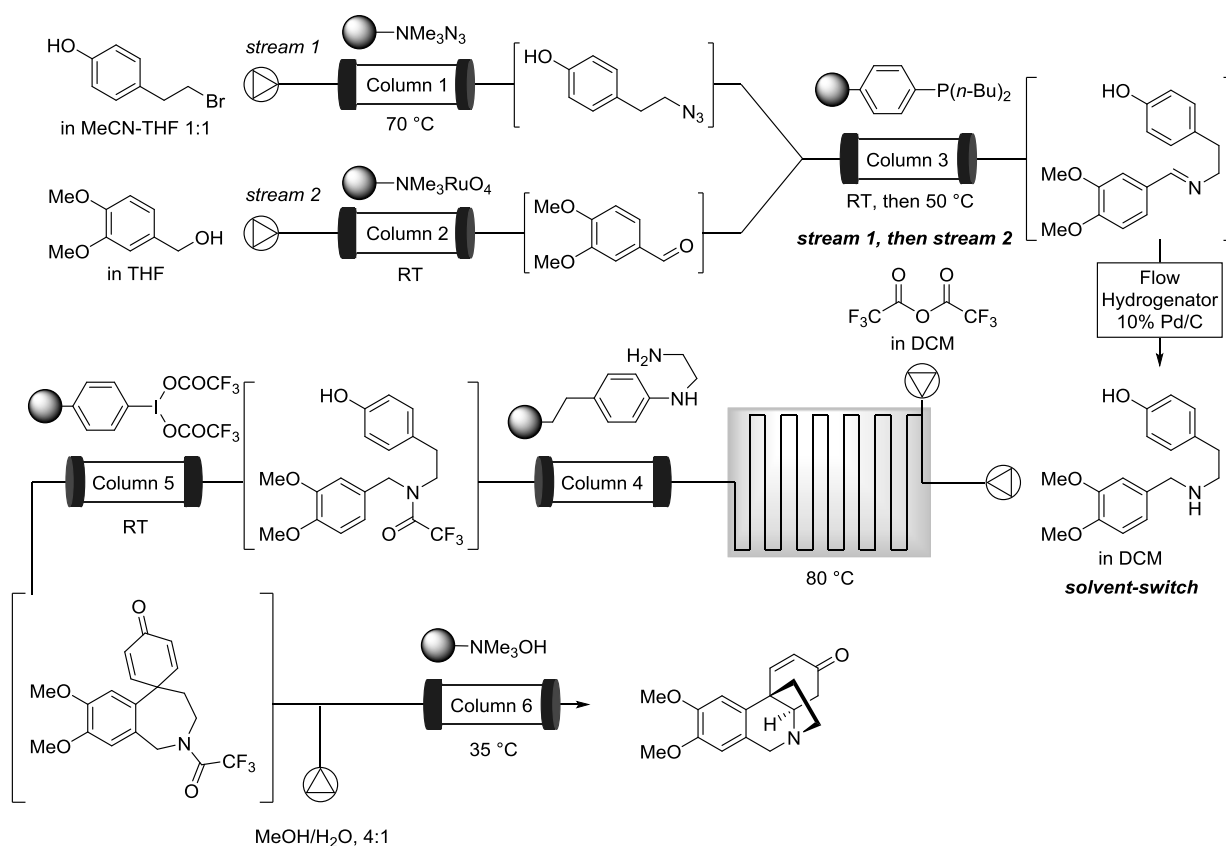


Next, an amine (stream 2) was passed through the column (Column 1) to react with a supported ester and an amide intermediate was formed. This first step reaction can be classified into the Type II reaction. The second column (Column 2) played a role in removing an unreacted amine. After the amide solution passing through the second column (Column 2), the third column (Column 3) containing silica-supported enzyme enabled self-coupling of the amide to give the desired compound, grossamide. The second step reaction can be defined the Type IV reaction.



**Scheme 1-2-1. Continuous flow synthesis of grossamide**

Though the first report consists of a 2-step reaction, more complicated flow syntheses have been reported so far. In 2006, S.V. Ley and co-workers reported 7-step flow synthesis of oxomaritidine (Scheme 1-2-2).<sup>11</sup> In the first step, a stream of an azide compound, which was synthesized from a commercially available alkyl bromide by the Type II reaction (Column 1), was introduced into the next column (Column 3) packed with a polymer-supported phosphine. Then, the corresponding aza-Wittig intermediate was formed and trapped in the next column (Column 3). This intermediate reacted with an aldehyde, which was prepared by an oxidation flow (Column 2), to give an imine product. Its hydrogenation afforded an amine compound, and at this stage, solvent exchange from THF to DCM was performed. And then, trifluoroacetylation of the corresponding amine gave an amide compound. In this Type I reaction, an excess amount of trifluoroacetic acid anhydride (TFAA) was employed, so Column 4 was inserted to catch the excess TFAA and residual trifluoroacetic acid (TFA). The stream following this scavenger column (Column 4) was connected to the next column (Column 5) containing polymer-supported (ditrifluoroacetoxyiodo)benzene (PS-PIFA), and cyclization proceeded to give a seven-membered tricyclic intermediate. Finally, polymer-supported base (Column 6) promoted cleavage of an amide bond, and spontaneously 1,4-addition took place to yield oxomaritidine. Therefore one Type I reaction, five Type II reactions, and one Type IV reaction were contained in this synthesis. Although solvent exchange was required during this synthesis, this report showed a possibility to prepare a compound with complicated structure using flow methods.



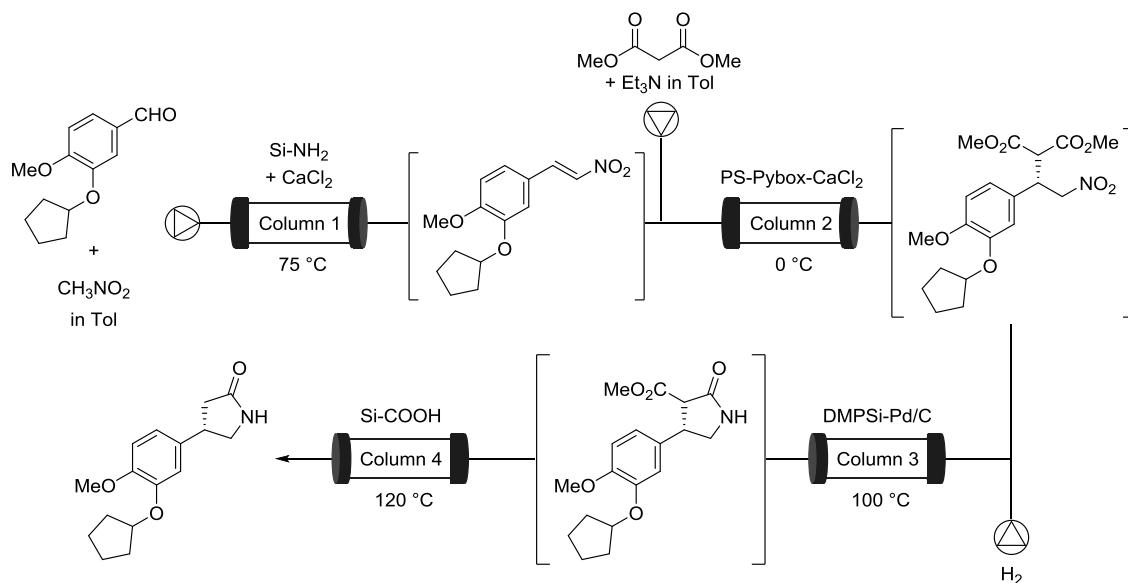
**Scheme 1-2-2. Continuous flow synthesis of oxomartidine**

In addition to the above examples, a variety of fine chemicals have been synthesized in continuous-flow manner, and some continuous-flow systems utilize in-line quenching and purification technologies.<sup>2,12-13</sup> Although such examples show advantages of flow methods, it can be said that they are just applications of traditional batch reactions. To eclipse a conventional batch process of fine chemical synthesis, further development of catalysis for a continuous-flow method is necessary.

### 1-3 Continuous-flow Reactions with Heterogeneous Catalysts

Among the four flow reaction types, the type IV reaction, continuous-flow reactions with heterogeneous catalysts, has superiority in terms of reaction efficiency.<sup>14</sup> Especially, when several flow reactions are connected, the type IV reaction displays its efficiency. If a reaction proceeds without harmful byproducts and leaching of a catalyst, a flow reaction can connect to another flow reaction directly.

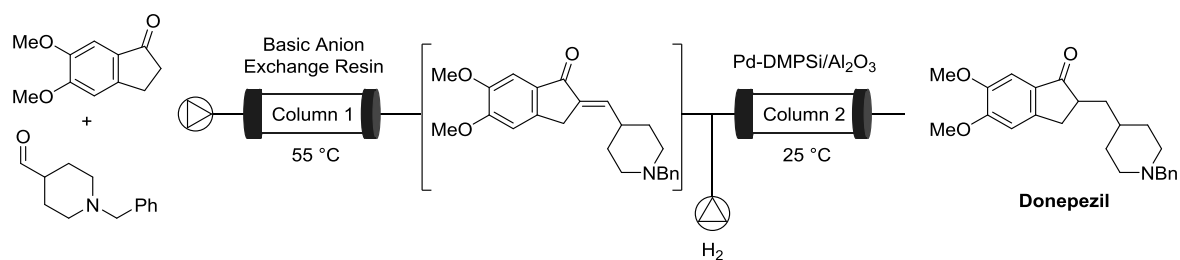
Our group focuses on development of the type IV reaction for continuous-flow synthesis of complex organic molecules. In 2015, multistep continuous-flow synthesis of (*R*)- and (*S*)-rolipram using only type IV continuous-flow systems have been achieved (Scheme 1-3-1).<sup>9</sup> This continuous-flow system was composed of four type IV reactions. In an initial step, nitroolefin was synthesized from an aldehyde and nitromethane catalyzed by amino-functionalized silica gel and  $\text{CaCl}_2$ . In the second step, enantioselective 1,4-addition of malonate to nitroolefin was performed by passing through a column reactor packed with a polystyrene supported pybox-calcium catalyst, which was developed by our group previously.<sup>15</sup> Hydrogenation of a nitro group and subsequent cyclization was catalyzed by a Pd supported catalyst to afford a lactam intermediate. Finally, carboxylic acid-functionalized silica gel promoted hydrolysis and decarboxylation to give the desired product in 50% yield in four step synthesis. These four reactions were connected without purification and solvent exchange.



**Scheme 1-3-1. Continuous flow synthesis of (*S*)-Rolipram**

Recently, our group has established the continuous-flow synthesis of Donepezil, which is a best-selling anti-Alzheimer's drug, with a two-step sequential-flow system (Scheme 1-3-2).<sup>16</sup> The first step is an aldol condensation reaction between an enolate of carbonyl compound and an aldehyde catalyzed by basic anion exchange resin. In the following step, alkene selective

hydrogenation was employed using our previously reported Pd catalyst.<sup>17</sup> The desired product was obtained selectively in 7.7 g per day for more than 30 hours.



**Scheme 1-3-2. Continuous-flow synthesis of Donepezil**

Thus far, there were a few examples related to continuous-flow synthesis with only type IV reaction besides rolipram and donepezil mentioned above.<sup>14</sup> Additionally, it has become usual to demonstrate a flow reaction with developed heterogeneous catalysts.

## 1-4 Heterogeneous Catalysts for Enantioselective Reactions

When we attempt to utilize the type IV reaction for synthesis of a variety of fine chemicals, an introduction of enantioselective reactions instead of kinetic resolutions in a synthetic process is unavoidable for the truly efficient synthesis. In order to perform enantioselective reactions with heterogeneous catalysts, chiral active species (e.g. chiral metal complexes or asymmetric organocatalysts) must be immobilized on support materials (e.g. polymers or inorganic materials). A common and reliable method to immobilize chiral active species is utilizing a covalent bond between a solid support and a chiral ligand or organocatalyst (Figure 1-4-1). A large number of heterogeneous catalysts prepared by this method have been reported,<sup>18-21</sup> and there are several examples of application for continuous-flow reaction.<sup>22</sup> Our group has also developed these types of heterogeneous catalysts previously, and the polystyrene-supported pybox-calcium catalyst used in the rolipram synthesis is one of the examples (Figure 1-4-2).<sup>15,23-26</sup> This catalyst was prepared by polymerization of functionalized pybox ligand and cross-linking monomers, and has the comparable activity to the corresponding homogeneous calcium catalyst.

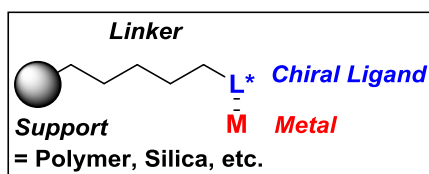


**Figure 1-4-1. Immobilization of chiral active species by utilizing covalent bonding**

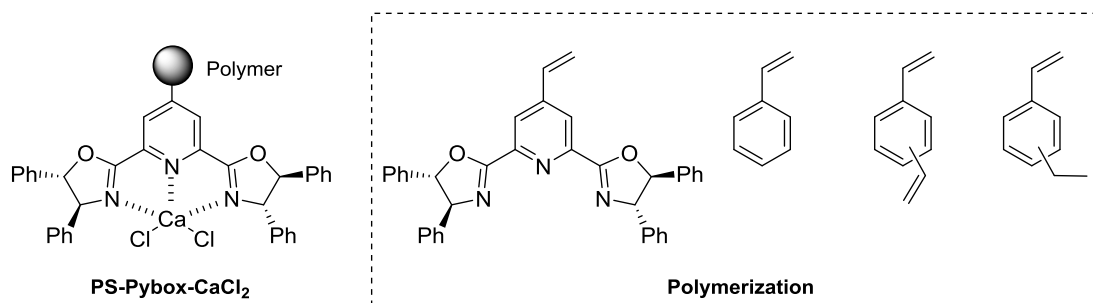


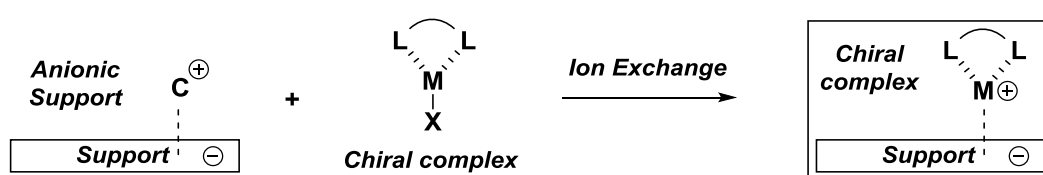
**Figure 1-4-2. Structure of PS-Pybox-CaCl<sub>2</sub>**

Generally, in the event that a chiral metal complex is immobilized in this way, chiral ligands functionalized on the supports have enough strong immobilization. In contrast, metal species has weaker interaction, which is coordination to the chiral ligands, and it would lead to leaching of metal species. Moreover, extra functionalization of a chiral ligand or an organocatalyst is required to immobilize on supports. For that reason, these types of heterogeneous catalysts often suffer from lower activity and selectivity than homogeneous catalyst. It takes time and effort to prepare functionalized chiral ligands or organocatalysts, and tuning of the catalyst structure is not easy.

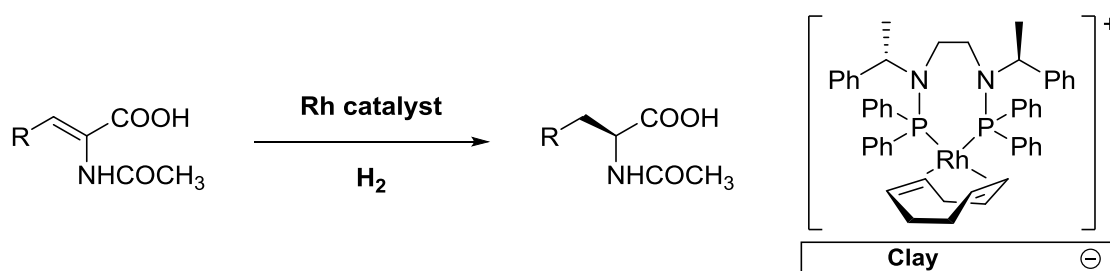
Another way to immobilize chiral active species on the supports is employing noncovalent bonding between solid supports and chiral active species.<sup>27</sup> Various kinds of heterogeneous catalysts

prepared by this method have been reported even though there are less examples compared to covalent bonding immobilization, and we could classify the noncovalent bonding immobilization into several types according to interaction modes between supports and chiral active species.

The first type is the immobilization utilizing an electrostatic interaction between a chiral complex and a support material. Commonly, an anionic solid material, which is clays, cation exchanged resins, zeolites and aluminasilicates, is employed as a support, and a cationic chiral metal complex is immobilized by ion exchange (Scheme 1-4-1). The first example reported in 1980 was the immobilization of a Rh complex on different clays. This heterogeneous catalyst was tested in the hydrogenation, and it could be recovered and reused for 5 runs with maintaining enantioselectivity (Scheme 1-4-2).<sup>28</sup>



**Scheme 1-4-1. Immobilization by electrostatic interaction**



**Scheme 1-4-2. Enantioselective hydrogenation with immobilized Rh catalyst**

Another type of interaction is adsorption of a chiral complex to a support. It is difficult to immobilize a chiral complex by only physisorption due to a weak interaction on a support. In contrast, an immobilization of a chiral complex by hydrogen bonding has been developed (Figure 1-4-3). A representative interaction of this way is observed between a counter anion of a chiral complex and a hydrogen atom located on a support such as silanol moiety of silica gel (Figure 1-4-3a). A successful heterogeneous catalyst based on this immobilization has been reported by Toste group in 2015 (Scheme 1-4-3).<sup>29</sup> In this report, a cationic Au(I) complex was immobilized on the mesoporous silica, SBA-15, and this heterogeneous catalyst worked well for regio- and enantioselective lactonization reactions. Compared with an unsupported Au(I) complex, dramatic enhancement of regio- and enantioselectivities were observed. The introduction of a hydrogen acceptor moiety into ligand structure also leads to hydrogen bonding between the ligand and the polar support (Figure 1-4-3b).<sup>27</sup>

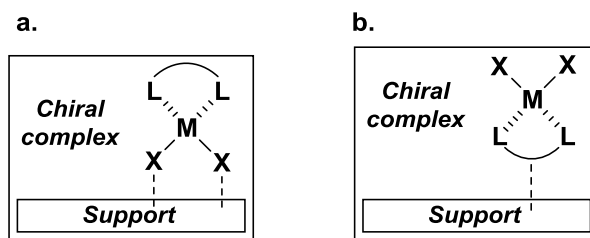
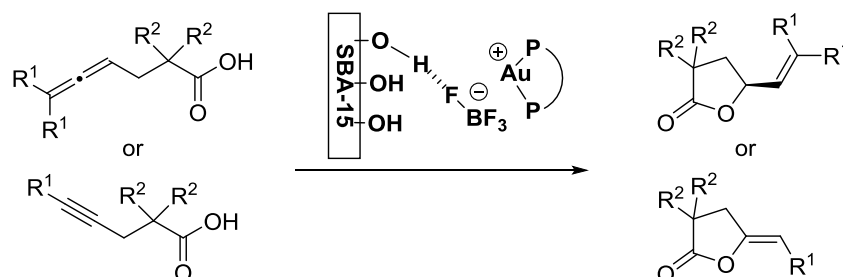


**Figure 1-4-3. Immobilization using hydrogen bonding**



**Scheme 1-4-3. Regio- and enantioselective lactonization reactions catalyzed by Au complex immobilized catalyst**

Entrapment of a chiral complex is known as another method of immobilization by noncovalent bonding (Figure 1-4-4).<sup>27</sup> In this way, a catalytic complex is enclosed inside structure of a support material, and no chemical interaction is found between a chiral complex and the support surface. As the support material, a flexible polymer or a rigid inorganic matrix are mainly employed. Using the former material, the main problem is leaching catalytic species caused by swelling of the polymer. This problem could be solved by utilizing the latter material, which requires a tunable cage in accordance with the size of metal complexes and reaction substrates.

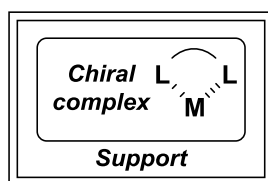


**Figure 1-4-4. Immobilization of a chiral complex by entrapment**

In recent years, heterogeneous catalysts that are prepared by self-assembly of active species have been reported.<sup>19,30</sup> In this way, no need of additional support and high density of active site is realized by solidification of the chiral catalyst itself. However, there are disadvantages: need of functionalization of the chiral ligand and difficulty of prediction of the structure.

As for the noncovalent immobilization described above, there are four types of interaction modes: electrostatic interaction, adsorption on the surface, entrapment into the structure, and self-assembly of chiral species. In these methods, support materials have an important role not only in the immobilization of chiral active species but also in the catalytic activity of immobilized

catalysts.

As a different approach to introduce a chiral active species on a support material, chiral modification of an immobilized metal species on a support surface is a known strategy (Figure 1-4-5).<sup>19</sup> Particularly, in metal nanoparticle chemistry, chiral heterogeneous catalysts based on this concept have been developed so far.<sup>31</sup> An early and representative example of this catalysis is asymmetric hydrogenation of methyl pyruvate or methyl benzoylformate catalyzed by cinchonidine-modified Pt on carbon, namely, Orito reaction in 1979 (Scheme 1-4-4).<sup>32-33</sup> In spite of remarkable studies of this catalysis, the development of chiral modification catalysis was limited for 20 years from the Orito's work. In the 2000s, several successful works have been reported mostly in asymmetric hydrogenation reactions.<sup>34</sup> Our group has developed this type of heterogeneous catalysts using Pd, Rh and Au as metal nanoparticles.<sup>31,35</sup> For instance, heterogeneous Rh nanoparticle immobilized on a nanocomposite of polystyrene-based copolymer with cross-linking moiety and carbon black showed catalytic activity for asymmetric 1,4-addition of boronic acids in the presence of a chiral diene ligand as a modifier.<sup>36</sup>

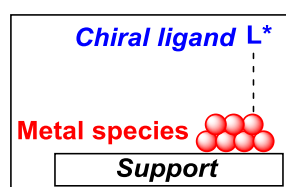
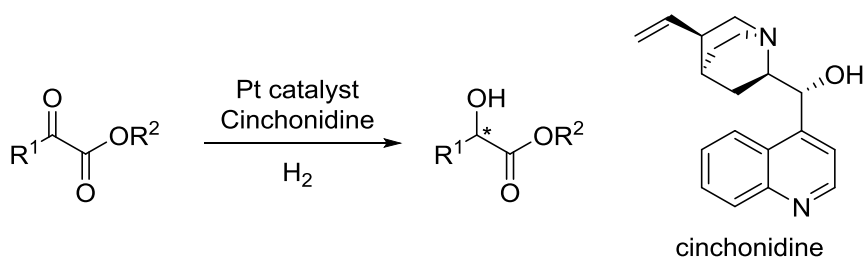


**Figure 1-4-5. Chiral modification of immobilized metal species**



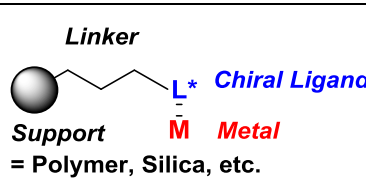
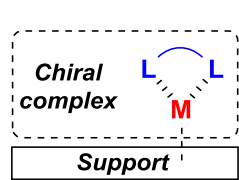
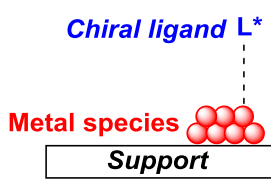
**Scheme 1-4-4. Orito reaction**

In this section, several methodologies to create asymmetric heterogeneous catalysts were introduced (Table 1-4-1). A common method is immobilization of a chiral ligand on a support material by functionalization of ligand structure, and a metal species is coordinated to a ligand moiety. To mimic a chiral environment in a homogeneous system, organic linkers have an important role in locating an active species far from a support surface. In general, it is difficult to achieve better activity and selectivity than those of a parent homogeneous catalyst due to an additional functionalization of the ligand structure, and it takes time and efforts to prepare such ligands. Immobilization by noncovalent bonding is much easier to prepare catalysts because homogeneous catalysts can be used for preparation. If a support material has a positive effect for catalysis, it is possible to attain better activity and selectivity than homogeneous catalysts. Due to weak interaction



between a chiral complex and a support material, however, there are less successful examples compared with covalent bonding immobilization. The third method is chiral modification of grafted metal species. In this method, a chiral ligand coordinates to a metal species immobilized on a support to afford a catalytic chiral active species on a support surface.

**Table 1-4-1. Summary of immobilization methods**

Method	Structure	Feature
<b>Covalent immobilization of Ligand</b>	 <p>Support = Polymer, Silica, etc.</p>	<ul style="list-style-type: none"> <li>➤ Common method</li> <li>➤ Troublesome preparation</li> <li>➤ Decreasing activity and selectivity</li> </ul>
<b>Noncovalent immobilization of chiral complex</b>		<ul style="list-style-type: none"> <li>➤ Less successful examples</li> <li>➤ Easy preparation</li> <li>➤ Weak interaction</li> </ul>
<b>Chiral modification to immobilized metal species</b>		<ul style="list-style-type: none"> <li>➤ Less successful examples</li> <li>➤ Easy preparation</li> <li>➤ Different species with homogeneous catalysts</li> </ul>

## 1-5 Design of Heterogeneous Catalysts for Continuous-flow Reactions

Comparing batch reactions and continuous-flow reactions with heterogeneous catalysts, there is a huge difference as for reaction environments. Normally, in batch reactions, liquid phase and solid phase are mixed by stirring, and substrates eventually contact with an active site immobilized on a support (Figure 1-5-1a). On the other hand, in continuous-flow reactions, liquid phase including substrates is passed through a column reactor packed with a heterogeneous catalyst, and substrates are frequently adsorbed and desorbed to solid surface (Figure 1-5-1b). Thus, due to higher frequency of adsorption of substrates to the solid surface compared with batch reactions, catalyst design utilizing the property of the support surface is suitable for continuous-flow reactions with heterogeneous catalysts. Among the immobilization methods introduced in the previous section, noncovalent immobilization of chiral complexes and chiral modification of immobilized metal species are preferable methods for continuous-flow reactions.

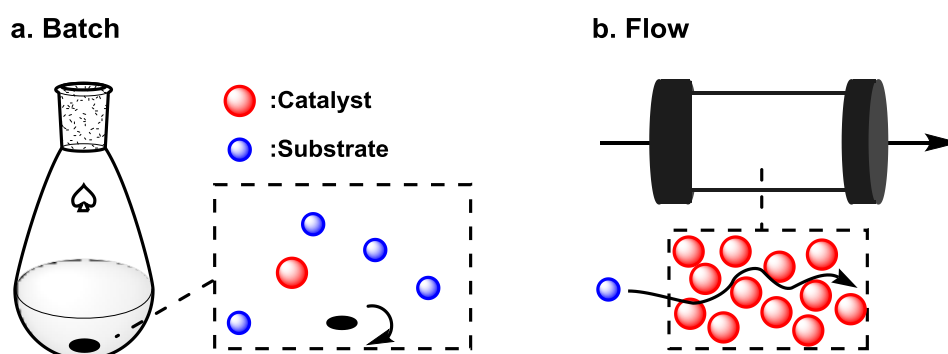


Figure 1-5-1. Reaction environment in batch and flow

## 1-6 References

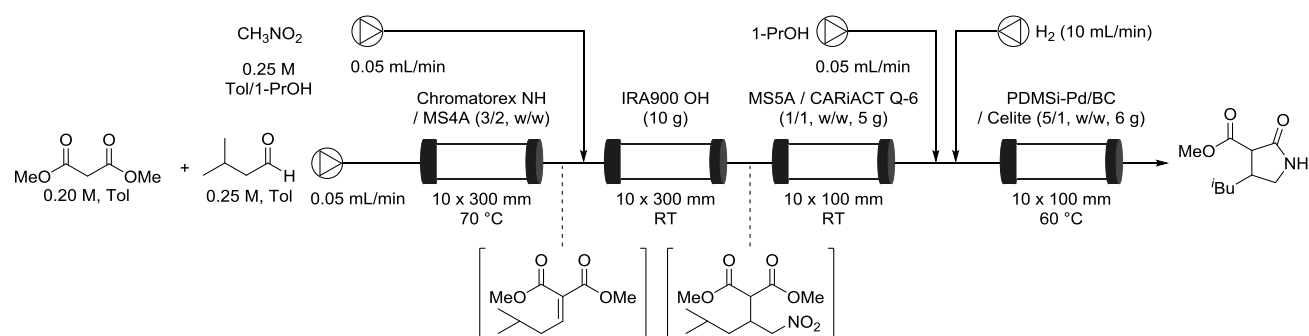
- (1) J. Wegner, S. Ceylan, A. Kirschning, *Adv. Synth. Catal.* **2012**, *354*, 17–57.
- (2) J. C. Pastre, D. L. Browne, S. V. Ley, *Chem. Soc. Rev.* **2013**, *42*, 8849–8869.
- (3) D. T. McQuade, P. Seeberger, *J. Org. Chem.* **2013**, *78*, 6384–6389.
- (4) Y. Su, N. J. W. Straathof, V. Hessel, T. Noële, *Chem. Eur. J.* **2014**, *20*, 10562–10589.
- (5) S. Kobayashi, *Chem. Asian. J.* **2016**, *11*, 425–436.
- (6) R. L. Hartman, J. P. McMullen, K. F. Jensen, *Angew. Chem. Int. Ed.* **2011**, *50*, 7502–7519.
- (7) C. Wiles, P. Watts, *Green Chem.* **2012**, *14*, 38–54.
- (8) J. Yoshida, *Chem. Rec.* **2010**, *10*, 332–341.
- (9) T. Tsubogo, H. Oyamada, S. Kobayashi, *Nature* **2015**, *520*, 329–332.
- (10) I. R. Baxendale, C. M. Griffiths–Jones, S. V. Ley, G. K. Tranmer, *Synlett* **2006**, *3*, 427–430.
- (11) I. R. Baxendale, J. Deeley, C. M. Griffiths–Jones, S. V. Ley, S. Saaby, G. K. Tranmer, *Chem. Commun.* **2006**, 2566–2568.
- (12) S. Mascia, P. L. Heider, H. Zhang, R. Lakerveld, B. Benyahia, P. I. Barton, R. D. Braatz, C. L. Cooney, J. M. B. Evans, T. F. Jamison, K. F. Jensen, A. S. Myerson, B. L. Trout, *Angew. Chem. Int. Ed.* **2013**, *52*, 12359–12363.
- (13) J. Britton, C. L. Raston, *Chem. Soc. Rev.* **2017**, *46*, 1250–1271.
- (14) K. Masuda, T. Ichitsuka, N. Koumura, K. Sato, S. Kobayashi, *Tetrahedron*, **2018**, *74*, 1705–1730.
- (15) T. Tsubogo, Y. Yamashita, S. Kobayashi, *Chem. Eur. J.* **2012**, *18*, 13624–13628.
- (16) B. Laroche, Y. Saito, H. Ishitani, S. Kobayashi, *Org. Process Res. Dev.* **2019**, *23*, 961–967.
- (17) S. Kobayashi, M. Okumura, Y. Akatsuka, H. Miyamura, M. Ueno, H. Oyamada, *ChemCatChem*, **2015**, *7*, 4025–4029.
- (18) J. M. Notestein, A. Katz, *Chem. Eur. J.* **2006**, *12*, 3954–3965.
- (19) M. Heitbaum, F. Glorius, I. Escher, *Angew. Chem. Int. Ed.* **2006**, *45*, 4732–4762.
- (20) S. Rostamnia, E. Doustkhah, *RSC Adv.* **2014**, *4*, 28238–28248.
- (21) M. Bartók, *Catal. Rev. - Sci. Eng.* **2015**, *57*, 192–255.
- (22) F. G. Finelli, L. S. M. Miranda, R. O. M. A. de Souza, *Chem. Commun.* **2015**, *51*, 3708–3722.
- (23) J. Miguez, H. Miyamura, S. Kobayashi, *Adv. Synth. Catal.* **2017**, *359*, 2897–2900.
- (24) T. Kuremoto, T. Yasukawa, S. Kobayashi, *Adv. Synth. Catal.* **2019**, *362*, 3698–3703.
- (25) H. Min, H. Miyamura, T. Yasukawa, S. Kobayashi, *Chem. Sci.* **2019**, *10*, 7619–7626.
- (26) T. Yasukawa, R. Masuda, S. Kobayashi, *Nat. Catal.* **2019**, *2*, 1088–1092.
- (27) J. M. Fraile, J. I. Garcia, J. A. Mayoral, *Chem. Rev.* **2009**, *109*, 360–417.
- (28) M. Mazzei, W. Marconi, M. Riocci, *J. Mol. Catal.* **1980**, *9*, 381–387.
- (29) X.-Z. Shu, S. C. Nguyen, Y. He, F. Oba, Q. Zhang, C. Canlas, G. A. Somorjai, A. P. Alivisatos, F. D. Toste, *J. Am. Chem. Soc.* **2015**, *137*, 7083–7086.
- (30) A. V. Artem'eva, V. P. Fedin, *Russ. J. Org. Chem.* **2019**, *55*, 901–922.
- (31) T. Yasukawa, H. Miyamura, S. Kobayashi, *ACS Catal.* **2016**, *6*, 7979–7988.

- (32) Y. Orito, S. Imai, S. Niwa, G. H. Nguyen, *Yuki Gosei Kagaku Kyokaiishi* **1979**, *37*, 173–174.
- (33) Y. Orito, S. Imai, S. Niwa, *Nippon Kagaku Kaishi* **1979**, 1118–1120.
- (34) F. Meemken, A. Baiker, *Chem. Rev.* **2017**, *117*, 11522–11569.
- (35) H. Miyamura, K. Nishino, T. Yasukawa, S. Kobayashi, *Chem. Sci.* **2017**, *8*, 8362–8372.
- (36) T. Yasukawa, H. Miyamura, S. Kobayashi, *J. Am. Chem. Soc.* **2012**, *134*, 16963–16966.

## Chapter 2. Chiral Nickel Diamine Complexes Immobilized on Mesoporous Silica for Asymmetric 1,4-Addition Reactions

### 2-1 Background and Strategy

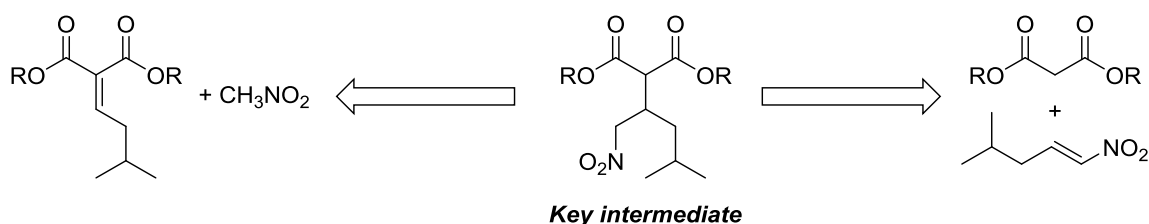
Previously, 3-steps sequential-flow synthesis of racemic pregabalin, which is one of the  $\gamma$ -aminobutyric acid (GABA) derivatives and one of the world's top-selling drugs used for the treatment of various ailments, such as epilepsy, neuropathic pain, anxiety disorder, etc., was investigated (Scheme 2-1-1).<sup>1</sup> In this continuous-flow synthesis, Knoevenagel condensation with isovaleraldehyde and dimethylmalonate was employed as the first step catalyzed by primary amine functionalized silica gel (Chromatorex NH) packed in a column reactor to afford alkylidene malonate. The stream eluted from the first step was mixed with a nitromethane solution, and flowing the mixture into a reactor packed with strongly basic anion exchange resin catalyst (Amberlite IRA900 OH) allowed the 1,4-addition reaction of nitromethane to alkylidene malonate to proceed efficiently. Subsequently, the intermediate obtained in the second step was passed through the third column reactor packed with a Pd catalyst with hydrogen gas as a third step. In this step, hydrogenation of the nitro group followed by cyclization gave the  $\gamma$ -lactam that is a precursor of pregabalin. This sequential-flow system worked well to afford the desired product in 75-100% yield in 3 steps for 45 h operation. The precursor of pregabalin could be easily transformed to pregabalin by an acid treatment according to a literature method.<sup>2</sup> As described here, continuous-flow synthesis of racemic pregabalin has been achieved. However, since the actual drug is a chiral compound, an enantioselective continuous-flow synthesis of pregabalin with a chiral heterogeneous catalyst is required to carry out a highly efficient synthetic process.



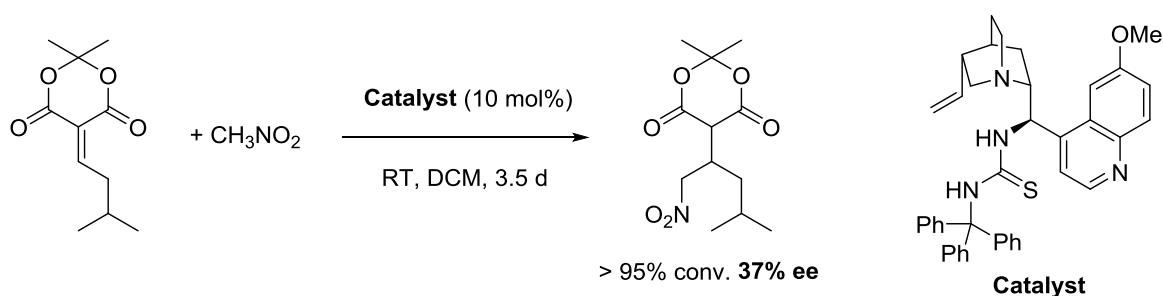
**Scheme 2-1-1. Continuous-flow synthesis of a precursor of racemic pregabalin**

To accomplish the enantioselective continuous-flow synthesis, a key intermediate must be prepared in an enantioselective manner. In the racemic synthesis, that intermediate was synthesized by 1,4-addition of nitromethane to alkylidene malonate (Scheme 2-1-2). However, there were no successful examples regarding enantioselective synthesis by this synthetic route. Koskinen group tried to apply a thiourea type organocatalyst into 1,4-addition reactions of a nitromethane to an alkylidene malonate derived from Meldrum's acid, and the reaction slowly proceeded to give the

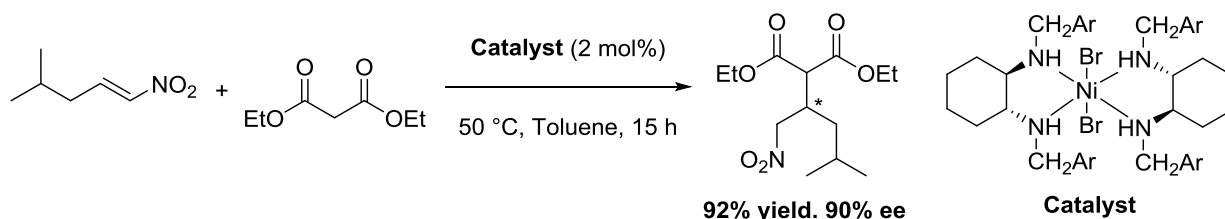
product with 37% ee (Scheme 2-1-3).<sup>3</sup> Meanwhile, the key intermediate could be prepared by 1,4-addition of malonates to nitroalkenes (Scheme 2-1-2). As for the enantioselective synthesis from these substrates, there were several successful examples utilizing organocatalysts<sup>2,4-10</sup> and metal complex catalysts.<sup>11-13</sup> Although efficient chiral Lewis acid catalysts were rare for the reactions with nitroalkenes bearing aliphatic substituents, Evans group has reported that a Ni(II)-diamine complex was shown to catalyze 1,4-addition reactions of 1,3-dicarbonyl compounds with a wide range of nitroalkenes including aliphatic substrates in high yields with good selectivities (Scheme 2-1-4).



**Scheme 2-1-2. Two different routes for synthesis of the key intermediate**



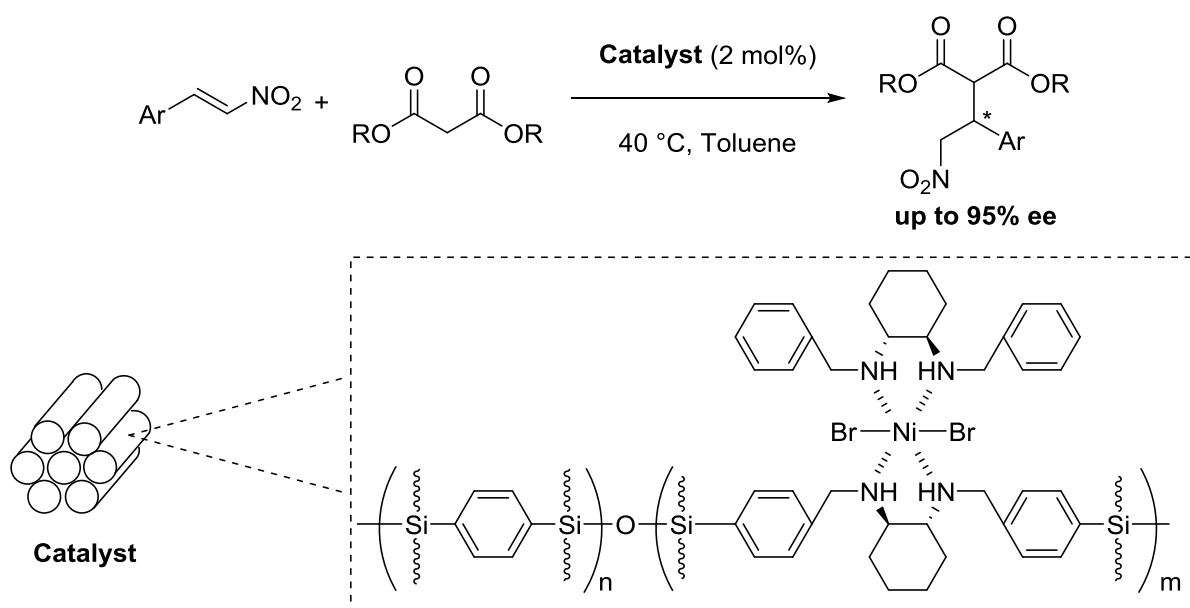
**Scheme 2-1-3. Trial of enantioselective 1,4-addition of nitromethane by thiourea catalyst**



**Scheme 2-1-4. Example of enantioselective 1,4-addition of malonate by Ni(II)-diamine catalyst**

To develop an asymmetric 1,4-addition reaction catalyzed by a heterogeneous catalyst, immobilization of Ni chiral active species on a solid support is required. Asymmetric reactions catalyzed by heterogeneous Ni catalysts are not rare. In particular, enantioselective hydrogenation of methylacetoacetate utilizing heterogeneous Ni catalysts, which are generated by the modification of Ni species by chiral tartaric acid, is well developed.<sup>14</sup> However, there are limited examples of asymmetric C—C bond formation reactions using heterogeneous Ni catalysts.<sup>15-18</sup> As for immobilization of Ni(II) chiral diamine complexes, a heterogeneous catalyst has been developed

(Scheme 2-1-5).<sup>17-18</sup> In 2012, Liu and Li group prepared chiral diamine-immobilized mesoporous silica by copolymerization of a functionalized chiral ligand and a structure directing reagent. The prepared functionalized mesoporous silica captured a nickel(II) bromide coordinated by an additional chiral ligand to afford active chiral species. It can be said that this immobilization method is classified into covalent immobilization of ligand. This heterogeneous catalyst was active for enantioselective 1,4-addition of malonate to various nitroalkenes to give the corresponding products in good yields and selectivities, though they did not mention the applicability to nitroalkenes bearing aliphatic substituents. Moreover, this catalyst could not suppress Ni leaching during a reusability test; 18.4% of Ni was leached out after the tenth reuse.

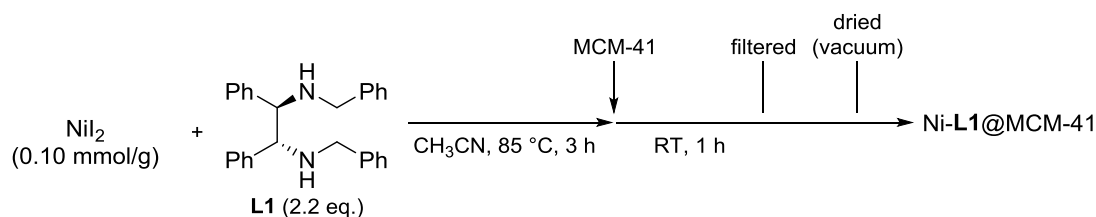


**Scheme 2-1-5. Example of enantioselective 1,4-addition of malonate by heterogeneous Ni(II)-diamine catalyst**

To develop a heterogeneous catalyst for enantioselective 1,4-addition reactions under continuous-flow conditions, immobilization of the Ni(II)-diamine complex was investigated. In this chapter, noncovalent immobilization of a chiral complex was attempted taking the efficiency of this method for continuous-flow reactions into account. To overcome a conventional problem of this method, weak interaction between a chiral complex and a support, a mesoporous silica gel was utilized as a support material, which has a large surface area and unified and enough large pore size to capture the chiral complex.

## 2-2 Catalyst Preparation and Characterization

For the catalyst preparation, Ni(II) diamine complex (NiI<sub>2</sub>-2L1) solution was mixed with MCM-41, which is one of the mesoporous silica gels, then filtering and drying the heterogeneous catalyst (Scheme 2-2-1). Ni loading of the prepared heterogeneous catalysts was determined by ICP analysis after dissolving the catalysts by addition of HF aqueous solution. When target loading of Ni was 0.1 mmol/g, actual loading was around 0.065 mmol/g.

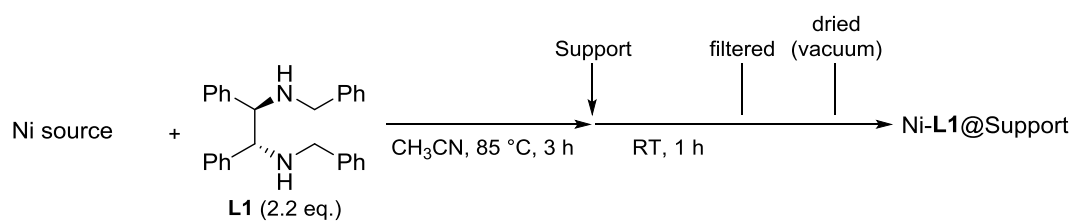


**Scheme 2-2-1. Preparation of the chiral heterogeneous catalyst**

Conditions of the catalyst preparation were examined as shown in Table 2-2-1. Instead of MCM-41, an amorphous silica gel (CARIACT Q-30) and molecular sieves 4 A were used as a support material, and lower loading rates of Ni were observed (Entry 1 and 2). It was necessary that both the mesoporous structure and the property of silica gel for immobilization of Ni species. Counter anions of Ni source have an important role on immobilization of metal species. When NiBr<sub>2</sub> and NiCl<sub>2</sub> were employed alternatively, loading rates also decreased to around 30% (Entry 4 and 5). Increasing the target loading to 0.202 and 0.435, actual loading reached a saturation point (Entry 7 and 8). With prepared different loading catalysts, nitrogen adsorption experiments were performed. The typical type IV isotherm of MCM-41 was also observed for Ni-L1@MCM-41, which indicated that the hexagonal mesoporous structure was maintained (Figure 2-2-1). Moreover, the decrease in the BET surface area and pore volumes of the catalyst embedded samples suggested that some adsorbents are partially blocking the pores, while the external surface was globally constant, which strongly suggested that Ni-L1 complexes were located within the mesopores of MCM-41 (Table 2-2-2).

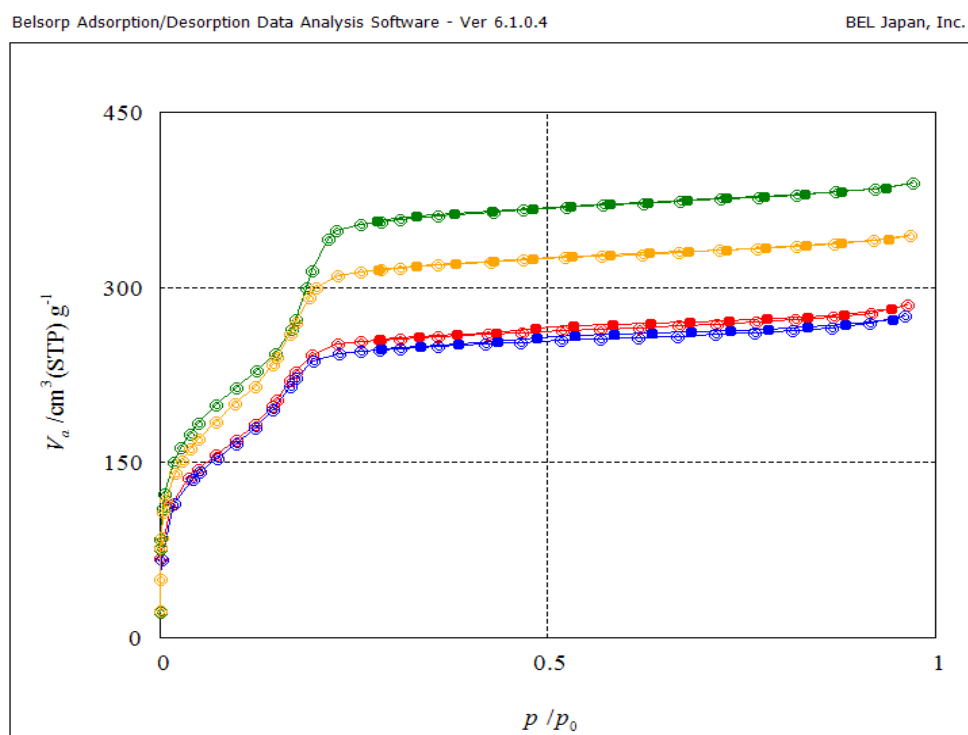


**Table 2-2-1. Investigation of conditions for catalyst preparation**



Entry	Ni source	Support	Target loading [mmol/g]	Actual loading <sup>a</sup> [mmol/g]	Loading rate [%]
1	NiI <sub>2</sub>	CARiACT Q-30	0.049	0.012	24
2	NiI <sub>2</sub>	MS4A	0.049	0.013	27
3	NiI <sub>2</sub>	MCM-41	0.050	0.039	78
4	NiBr <sub>2</sub>	MCM-41	0.101	0.035	34
5	NiCl <sub>2</sub>	MCM-41	0.112	0.031	28
6	NiI <sub>2</sub>	MCM-41	0.098-0.113	0.063-0.073	59-73
7	NiI <sub>2</sub>	MCM-41	0.202	0.111	55
8	NiI <sub>2</sub>	MCM-41	0.435	0.153	35

<sup>a</sup>The amount of nickel was determined by ICP analysis.



**Symbols:** MCM-41 (**green**); Ni-L1@MCM-41-a (**yellow**); Ni-L1@MCM-41-b (**red**);  
Ni-L1@MCM-41-c (**blue**)

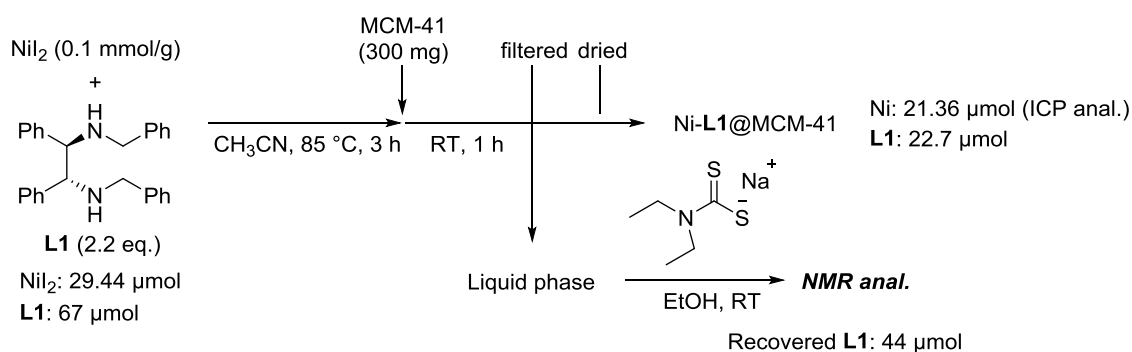
**Figure 2-2-1.** Isotherm of MCM-41 and Ni-L1@MCM-41

**Table 2-2-2.** Changes of the pore structure of Ni-L1@MCM-41<sup>a</sup>

Sample	Actual loading (mmol/g)	BET surface area (m <sup>2</sup> /g)	External surface area (m <sup>2</sup> /g)	Internal surface area (m <sup>2</sup> /g)	Pore volume (cm <sup>3</sup> /g)
MCM-41	0	952.7	100.2	852.5	0.6029
Ni-L1@MCM-41-a	0.064	823.6	102.9	720.6	0.5334
Ni-L1@MCM-41-b	0.111	677.3	100.4	576.9	0.4411
Ni-L1@MCM-41-c	0.153	650.4	100.0	550.5	0.4262

<sup>a</sup>Surface area and pore volume were calculated by the BET method. The external surface area was determined by the T-plot method.

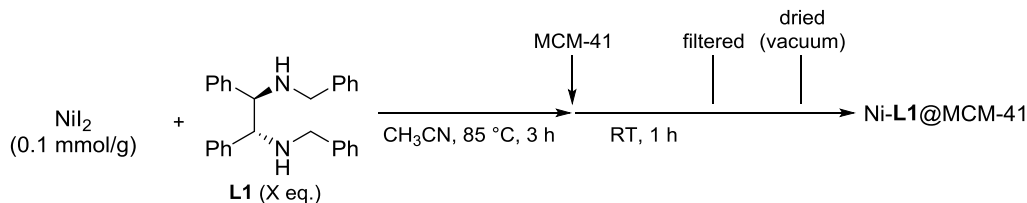
To clarify what species located on the support, further analysis of recovered solution during the catalyst preparation was performed. Since recovered solution from filtration might be contained Ni complex which was not detectable in <sup>1</sup>H NMR analysis due to paramagnetic property, Ni scavenger (diethyldithiocarbamate) was added to the solution to release free chiral diamine ligand, H NMR analysis determined the amount of chiral ligand in the solution (Scheme 2-2-2). As a result, 66% of the chiral ligand could be recovered, which revealed that 1.06 equivalent of chiral ligand for Ni species located on the support was immobilized. Also, iodine was quantified by ICP analysis of dissolved heterogeneous catalyst, and it was found that the heterogeneous contained 0.8 equivalent of iodine for Ni species. Therefore, it was indicated that different Ni species from homogeneous NiI<sub>2</sub>-2L1 complex was generated by immobilization on the support material.

**Scheme 2-2-2.** Detection of non-immobilized chiral ligand

After seeing these results, ligand amount used in catalyst preparation was investigated (Table 2-2-3). When homogeneous NiI<sub>2</sub>-L1 (1:1) complex was used as a parent complex for immobilization instead of NiI<sub>2</sub>-2L1 (1:2) complex, interestingly, significant decreasing of Ni loading was shown and almost chiral ligand was washed out from the support (entry 2). On the other hand, using 3.3 equivalents of chiral ligand afforded better Ni loading rate, however, the ratio of Ni and chiral ligand

was still 1:1 (entry 3). This result suggested that Ni-**L1** complex was stabilized on the support while such homogeneous complex is known to be unstable compared with NiI<sub>2</sub>-2**L1** complex.<sup>13</sup>

**Table 2-2-3. Investigation of ligand amount for catalyst preparation**



Entry	X	Target loading [mmol/g]	Actual loading <sup>a</sup> [mmol/g]	Loading rate [%]	L1/Ni
1	2.2	0.098-0.113	0.063-0.073	59-73	1.06
2	1.1	0.100	0.019	19	0.04
3	3.3	0.100	0.081	81	1.04

<sup>a</sup>The amount of nickel was determined by ICP analysis.

To further clarify Ni species immobilized on the surface of MCM-41, XAFS analysis of Ni-**L1**@MCM-41 was conducted. Visual inspection of the changes in the peak shapes of the Ni K-edge XANES spectra of NiI<sub>2</sub>-2**L1** and Ni-**L1**@MCM-41 suggested that the local structure of the immobilized catalyst was changed and is more in line with NiO than NiI<sub>2</sub> (Figure 2-2-2a), while the decrease in peak intensity in the pre-edge region implied an increase in the coordination number of Ni (Figure 2-2-2b). Based on Ni K-edge EXAFS spectral analysis, five oxygen and/or nitrogen atoms were identified in the primary coordination sphere, one oxygen or nitrogen atom in the second sphere, and one iodine atom in the outer sphere of the nickel complex (Figure 2-2-3a and b). With these results, we proposed the structure of Ni species located and stabilized inside the mesopore of MCM-41 (Figure 2-2-3c).

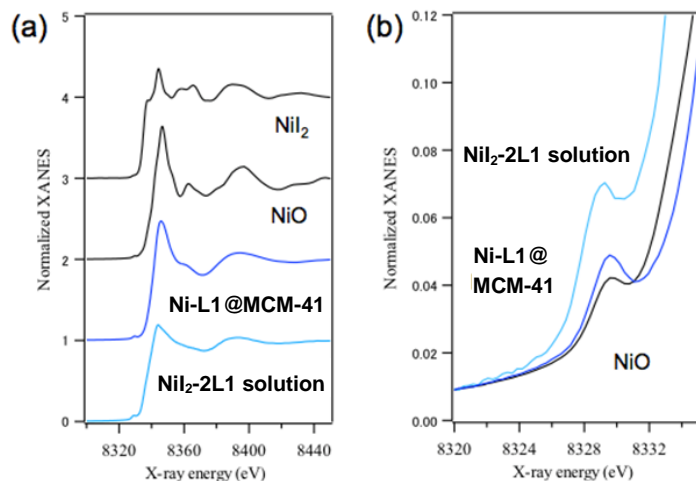


**Figure 2-2-2. a) Ni K-edge XANES spectra of NiI<sub>2</sub>, NiO, Ni-L1@MCM-41, and NiI<sub>2</sub>-2L1; b) Pre-edge structure of the Ni K-edge XANES spectra in Figure 2-2-2a.**

(a)	Shell	Coordination number	R/ Å	dE (ev)	DW
	Ni-O(N)	4.8	2.06	0	0.07
	Ni-O(N)	1.4	2.72	0.5	0.07
	Ni-I (theoretical)	0.6	2.86	0	0.07
	Ni-Si (theoretical)	2.2	3.32	0	0.07

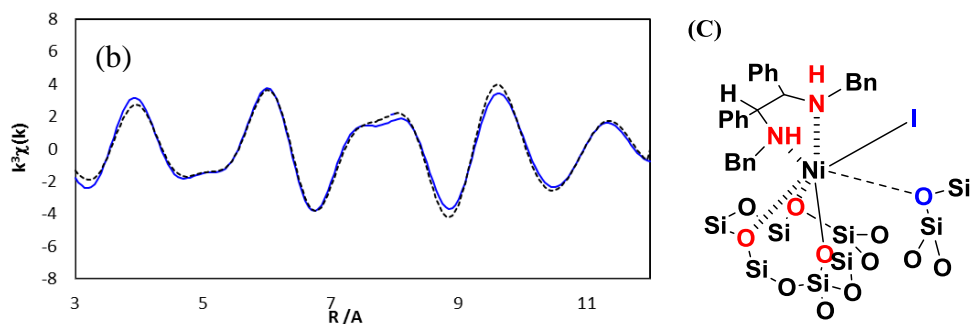


**Figure 2-2-3. a) Coordination mode around Ni after curve fitting; b) EXAFS fitting result; c) Proposed catalytic species within the mesopores of MCM-41.**

Finally, EDS mapping of the heterogeneous catalyst (Ni-L1@MCM-41) showed no detectable Ni on the support material, which indicated that Ni species highly dispersed on the surface of MCM-41 without any aggregation of Ni species (Figure 2-2-4).

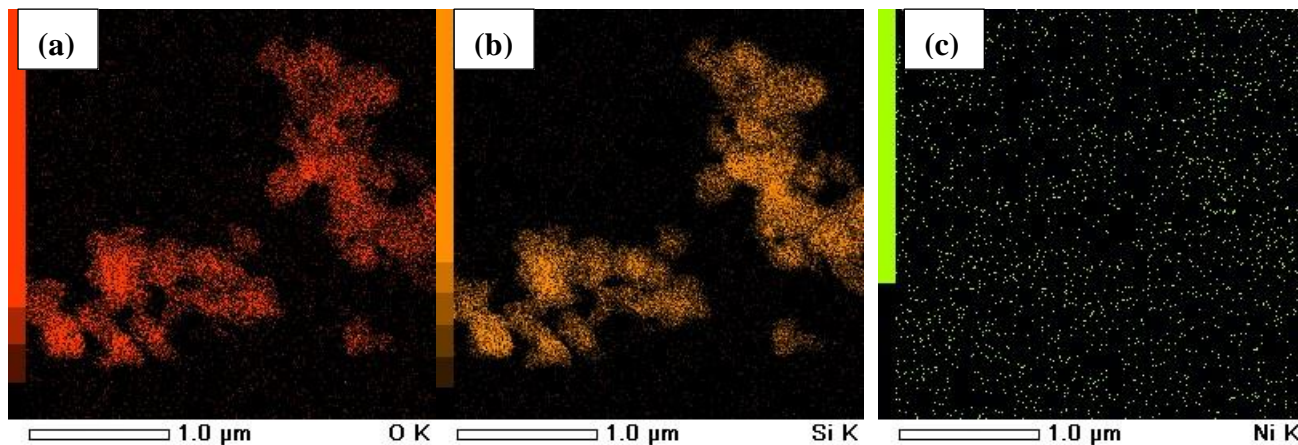


**Figure 2-2-4. EDS mapping of (a) Oxygen (b) Silicon (c) Nickel.**

### 2-3 Evaluation of Catalysts with 1,4-Addition of Malonate to Nitroalkene

In this section, optimization and evaluation of the heterogeneous catalyst with enantioselective conjugated addition of malonates to nitroalkenes was described. Firstly, optimization of chiral ligand was performed (Table 2-3-1). Although Evans group utilized *N,N'*-dibenzylcyclohexane-1,2-diamine (**L2**) as an optimal chiral ligand in referenced previous report,<sup>12,13</sup> employing **L2** instead of **L1** for the preparation of heterogeneous catalysts gave lower activity and enantioselectivity in 1,4-addition reaction of dimethylmalonate (**1a**) to nitroalkene (**2a**). When several catalysts were prepared with different chiral ligands (**L3-L6**) and tested for the catalysis (entries 3–6), no major difference was observed which indicated that the 1,2-diphenylethane-1,2-diamine structure was much suitable for the heterogeneous catalysts than reported ligand in homogeneous reactions. Moreover, solvent has a key role on this catalysis. In homogeneous reactions Evans reported, THF and DCE was also applicable for the catalysis, however, nonpolar solvent only afforded good result in with the heterogeneous catalyst (entries 1,7–8). I considered that polar substrates easily penetrated into mesopore of the catalyst in nonpolar solvent system, and the reaction occurred.

**Table 2-3-1. Examination of supported chiral nickel–diamine complexes as catalysts for enantioselective 1,4-addition of dimethyl malonate (**1a**) to nitroalkene (**2a**)** <sup>[a]</sup>

Ar = Ph, **L1**  
 = 4-Me-C6H4, **L3**  
 = 4-Br-C6H4, **L4**  
 = 1-naphthyl, **L5**  
 = 2-naphthyl, **L6**

Entry	Ln	Solvent	Yield [%] <sup>[b]</sup>	Ee [%] <sup>[c]</sup>
1	<b>L1</b>	Toluene	quant	90
2	<b>L2</b>	Toluene	70	80
3	<b>L3</b>	Toluene	95	88
4	<b>L4</b>	Toluene	quant	89
5	<b>L5</b>	Toluene	86	89
6	<b>L6</b>	Toluene	quant	90
7	<b>L1</b>	THF	25	86
8	<b>L1</b>	DCE	33	85

[a] Reaction conditions: **1a** (0.35 mmol), **2a** (0.25 mmol), and catalyst (1 mol%) in solvent (1.5 mL) at 60 °C for 12 h. [b] NMR yield using mesitylene as an internal standard. [c] Determined by chiral-phase HPLC analysis.

With the optimal condition in hand, substrate scope of the enantioselective 1,4-addition of dimethyl malonate (**1a**) with nitroalkenes (**2a–p**) was investigated (Table 2-3-2). It was found that various 2-substituted nitroalkenes (**2a–f**), bearing primary and secondary aliphatic moieties, were viable substrates that could undergo the asymmetric process to deliver  $\gamma$ -nitro bisesters (**3a–f**) in good to excellent yields with excellent enantioselectivities (entries 1–6). Furthermore, the more reactive  $\beta$ -nitrostyrenes (**2g–l**) could also be used as substrates for the asymmetric 1,4-addition reaction at room temperature (entries 7–9, 11–12) to provide excellent yields and enantioselectivities of the desired products (**3g–l**) with the exception of  $\beta$ -nitrostyrene **2j**, bearing an ortho-substituent, which required a slightly higher reaction temperature (entry 10). I also found that for electron-rich nitroolefin **2l**, a more Lewis acidic catalyst Ni-**L4**@MCM-41, was required and **3l** could be obtained in excellent yield with good enantioselectivity (entry 12). I also found that  $\beta$ -nitroalkenes bearing naphthyl (**2m**) and heteroaromatic (**2n–o**) moieties were good acceptors, providing the desired products **3m–o** in excellent yields and good to excellent enantioselectivities (entries 13–15). Furthermore, when conjugated nitroalkene **2p** was examined as a substrate, it was found that the 1,4-adduct **3p** could be exclusively obtained in excellent yield and enantioselectivity (entry 16).

**Table 2-3-2. Substrate scope of enantioselective 1,4-addition of dimethyl malonate (**1a**) with nitroalkenes (**2a-p**).**

$\text{MeO}-\text{C}(=\text{O})-\text{CH}_2-\text{C}(=\text{O})-\text{OMe} + \text{R}-\text{CH}=\text{CH}-\text{NO}_2 \xrightarrow[\text{Toluene, Temp., 12-40 h}]{\text{Ni-L1@MCM-41 (Ni: 1mol\%)}}$

Entry	R	Temp. [°C]	Time [h]	Yield [%] <sup>[b]</sup>	Ee [%] <sup>[c]</sup>
1	<i>t</i> Bu ( <b>2a</b> )	60	12	89	90
2	<i>n</i> Pr ( <b>2b</b> )	60	20	88	89
3	<i>n</i> heptyl ( <b>2c</b> )	60	40	66	87
4	2-phenylethyl ( <b>2d</b> )	60	20	95	89
5	cyclohexyl ( <b>2e</b> )	60	40	77	89
6	3-pentyl ( <b>2f</b> )	60	20	94	88
7	Ph ( <b>2g</b> )	rt	20	98	90
8	4-Cl-C <sub>6</sub> H <sub>4</sub> ( <b>2h</b> )	rt	20	83	88
9	4-Me-C <sub>6</sub> H <sub>4</sub> ( <b>2i</b> )	rt	20	92	91
10	2-Me-C <sub>6</sub> H <sub>4</sub> ( <b>2j</b> )	50	20	64	91
11	4-MeO-C <sub>6</sub> H <sub>4</sub> ( <b>2k</b> )	rt	40	97	97
12 <sup>[d]</sup>	4-Me <sub>2</sub> N-C <sub>6</sub> H <sub>4</sub> ( <b>2l</b> )	rt	40	86	80
13	2-naphthyl ( <b>2m</b> )	rt	40	quant	90
14	2-thiophenyl ( <b>2n</b> )	rt	20	97	90
15 <sup>[d]</sup>	3-indolyl ( <b>2o</b> )	rt	40	90	73
16	(E)-CH=CHPh ( <b>2p</b> )	50	40	quant	86

[a] Reaction conditions: **1a** (0.35 mmol), **2a-p** (0.25 mmol), and catalyst (1 mol%) in Toluene (1.5 mL). [b] NMR yield using mesitylene as an internal standard. [c] Determined by chiral-phase HPLC analysis. [d] Ni-**L4**@MCM-41 was used as a catalyst.

To confirm that the reaction occurred on the support, a hot filtration test was carried out by the reaction of **1a** with **2g** using Ni-**L1**@MCM-41 (Figure 2-3-1). While the reaction without filtration proceeded well to afford the desired product **3g** in excellent yield for 20 h, removal of the heterogeneous catalyst at 3 h by filtration let the catalysis completely stopped. This result supported that the Ni bound to MCM-41 was the catalytically active species.



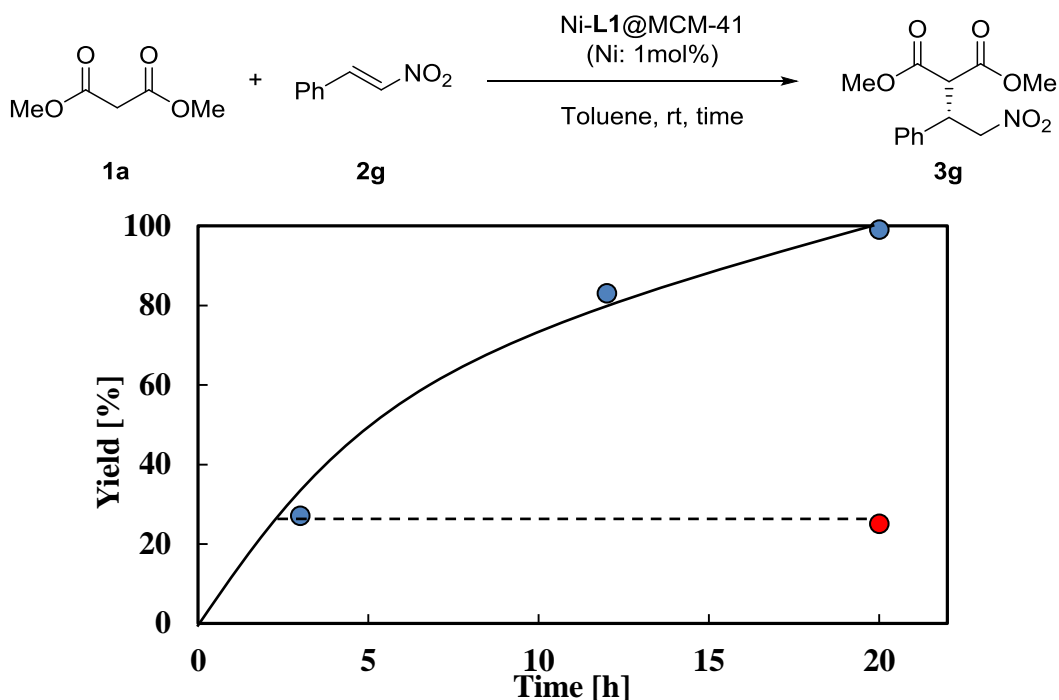


**Figure 2-3-1. Hot filtration test by enantioselective 1,4-addition of 1a with 2g**

Nitrogen adsorption experiments and the hot filtration test strongly indicated that catalytic active species was located inside the mesopore of MCM-41, which was supported by the relation between catalyst activity and size of substrates. I examined the reaction profiles for 1,4-addition of various malonates (**1a–d**) with nitroalkene (**2a**) catalyzed by the heterogeneous (Ni-L1@MCM-41) and homogeneous nickel complex (Ni<sub>2</sub>-L1) catalyst (Figure 2-3-2). When dimethyl malonate (**1a**) was used as a nucleophile substrate, the heterogeneous catalyst showed higher catalyst activity than the homogeneous complex. On the other hand, when the examination of the reaction profile with dibenzyl malonate (**1d**) was carried out, the homogeneous nickel complex led to better yields than the heterogeneous catalyst. These results indicated that the immobilized Ni species could attain higher catalyst activity by immobilization within the mesopore of MCM-41, however, bulky substrates had low frequency of penetrating into the catalytic active site to make the reaction slower.

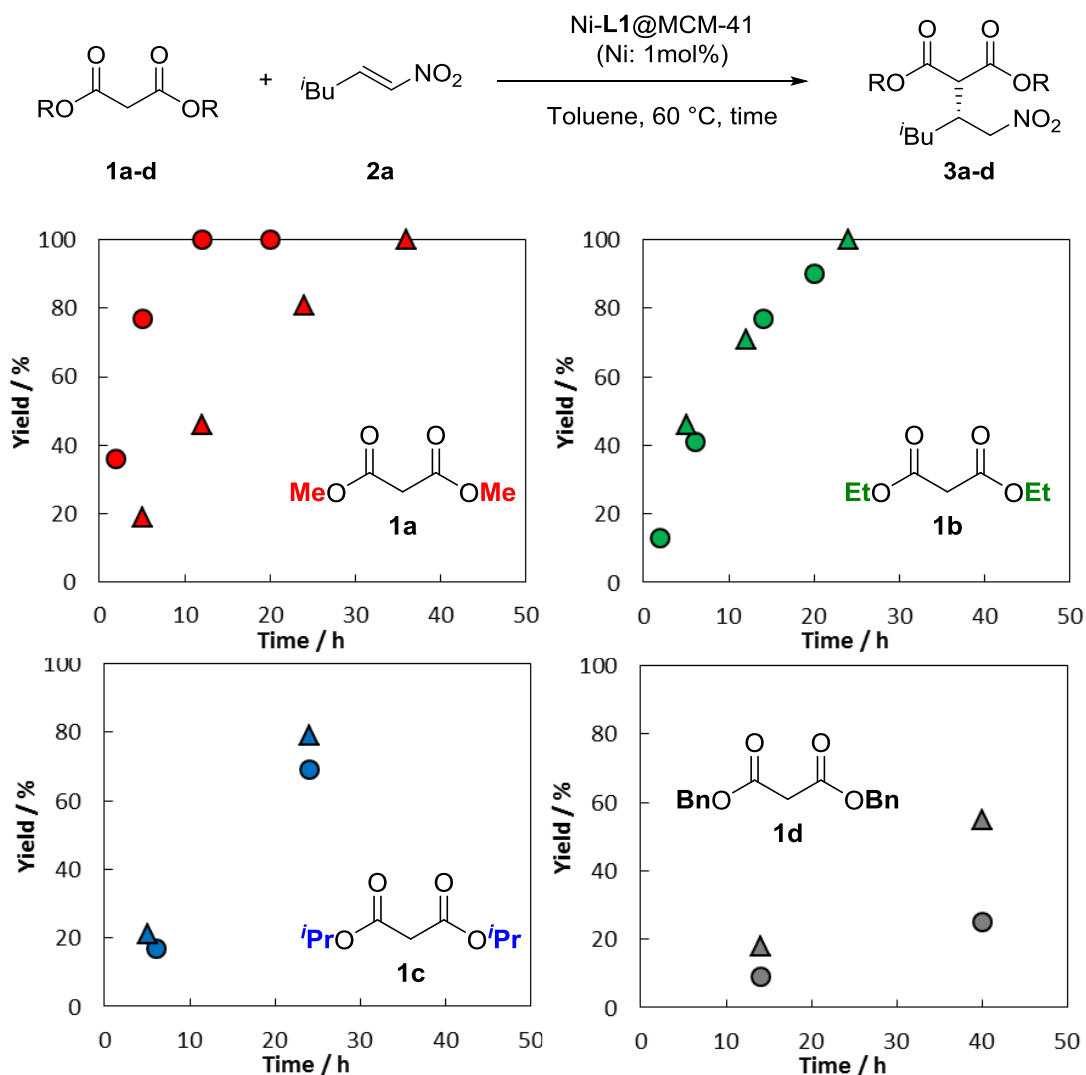


**Figure 2-3-2. Reactivity difference of dialkyl malonates 1a–1d with Ni-L1 (▲) and Ni-L1@MCM-41 (●) as catalysts. Yield was determined by NMR analysis.**

Reusability of the heterogeneous catalyst (Ni-L1@MCM-41) was investigated (Table 2-3-3). This catalyst could be recovered by simple filtration and reused three times without decreasing yield and enantioselectivity of the product (**3g**) though 6.6% of Ni leaching was observed in first reaction (Entry 1). When the experiments were conducted with shorter reaction time, the gradual decrease of the catalyst activity happened every time the catalyst was reused. I considered that the deactivation of the catalyst was mainly derived from the dissociation of the chiral ligand from Ni species rather than Ni leaching because leaching of the Ni species was suppressed from second run and hot filtration test indicated leached Ni species had little activity. In fact, the catalyst activity could be recovered by the use of additional chiral ligand (1 mol%) in forth run (Entry 2). Based on this result, I conducted the recovery and reuse studies by adding fresh **L1** after each run enabled the reuse of Ni-L1@MCM-41 up to three times without significant loss in the catalyst activity (Entry 3).

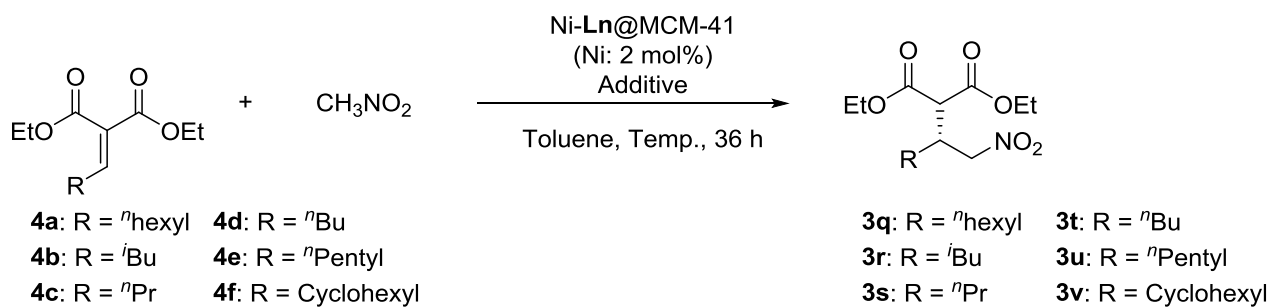


## 2-4 Investigation of 1,4-Addition of Nitromethane to Alkylidene Malonate

So far, I described that the developed heterogeneous catalyst had different nickel species from the homogeneous Ni complex located inside the mesopore of MCM-41. Here, other application of this catalyst for a challenging reaction was investigated. An alternative method to access enantiopure  $\gamma$ -nitro biesters (**3**) is through catalytic asymmetric conjugate addition reactions between nitromethane and alkylidene malonates. However, when alkylidene malonates, bearing aliphatic moieties, were used as substrates, the obtained enantioselectivities were poor or non-existent in previous reports as described in introduction part.

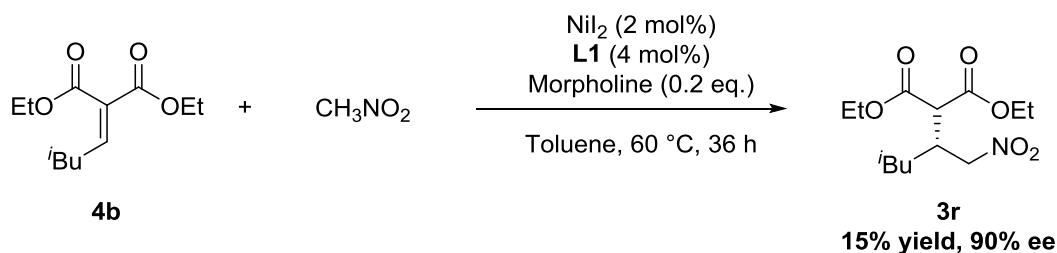
Firstly, when only Ni-**L1**@MCM-41 was employed for 1,4-addition of nitromethane with alkylidene malonate (**4a**), trace amount of the desired product (**3q**) was obtained due to low basicity of the heterogeneous catalyst (Table 2-4-1, entry 1). In order to promote deprotonation from nitromethane, various additives were investigated as an external base catalyst (entries 2-7). When tertiary amines were used as additives, the 1,4-adducts were obtained in low enantioselectivities (entries 2 and 6). Using secondary amines led to good enantioselectivities of the desired products, especially, the reaction with morpholine afforded the product in good yield and enantioselectivity (entry 5). Decreasing reaction temperature to 45 °C had no effect on the enantioselectivity (entry 8), and employing the different catalyst ([Ni-**L4**]@MCM-41), which has similar activity as standard catalyst (Ni-**L1**@MCM-41) for 1,4-addition reaction of malonates and nitroalkenes, caused lower yield of the product (entry 9). When the substrate **4b** which corresponds to the precursor of pregabalin was utilized, the reaction proceeded in good yield and enantioselectivity (entry 10). With this substrate further optimization was performed as for the catalyst and reaction solvent, significant enhancement of the yields and selectivities of the product were not observed (entries 11-13). This asymmetric 1,4-addition of nitromethane catalyzed by Ni-**L1**@MCM-41 and morpholine could proceed with various alkylidene malonates (**4c-f**), bearing aliphatic moiety, in good enantioselectivities (entries 14-17). Interestingly, it was shown that by conducting this asymmetric process with **4b** using catalytic amounts of NiI<sub>2</sub>-2**L1** provided  $\gamma$ -nitro ester **3r** in low yield, but with excellent enantioselectivity (Scheme 2-4-1).

**Table 2-4-1. Optimization of the condition for the enantioselective 1,4-addition of nitromethane to alkylidene malonates 4a-b<sup>a</sup>**



Entry	Substrate	Ln	Additive	Temp. [°C]	Yield [%] <sup>[b]</sup>	Ee [%] <sup>[c]</sup>
1	<b>4a</b>	<b>L1</b>	none	60	3	-
2	<b>4a</b>	<b>L1</b>	<sup>i</sup> Pr <sub>2</sub> NEt (0.2 eq.)	60	34	2
3	<b>4a</b>	<b>L1</b>	Piperidine (0.2 eq.)	60	53	78
4	<b>4a</b>	<b>L1</b>	Piperazine (0.2 eq.)	60	24	73
5	<b>4a</b>	<b>L1</b>	Morpholine (0.2 eq.)	60	80	83
6	<b>4a</b>	<b>L1</b>	<i>N</i> -methylmorpholine (0.2 eq.)	60	9	9
7	<b>4a</b>	<b>L1</b>	2,6-dimethylmorpholine (0.2 eq.)	60	44	79
8	<b>4a</b>	<b>L1</b>	Morpholine (0.2 eq.)	45	65	83
9	<b>4a</b>	<b>L4</b>	Morpholine (0.2 eq.)	60	54	84
10	<b>4b</b>	<b>L1</b>	Morpholine (0.2 eq.)	60	82	86
11	<b>4b</b>	<b>L4</b>	Morpholine (0.2 eq.)	60	79	84
12 <sup>[d]</sup>	<b>4b</b>	<b>L1</b>	Morpholine (0.2 eq.)	60	81	80
13 <sup>[e]</sup>	<b>4b</b>	<b>L1</b>	Morpholine (0.2 eq.)	60	85	79
14	<b>4c</b>	<b>L1</b>	Morpholine (0.2 eq.)	60	75	78
15 <sup>[f]</sup>	<b>4d</b>	<b>L1</b>	Morpholine (0.2 eq.)	60	79	83
16 <sup>[f]</sup>	<b>4e</b>	<b>L1</b>	Morpholine (0.2 eq.)	60	78	84
17	<b>4f</b>	<b>L1</b>	Morpholine (0.2 eq.)	60	37	79

[a] Reaction conditions: **4a** (0.25 mmol), **nitromethane** (0.5 mmol), additive and catalyst (2 mol%) in Tol (1.5 mL) for 36 h. [b] NMR yield using mesitylene as an internal standard. [c] Determined by chiral-phase HPLC analysis. [d] Cyclohexane was used as solvent. [e] Pentane was used as solvent. [f] 48 h.



**Scheme 2-4-1. Enantioselective 1,4-addition of nitromethane to alkyldiene malonate with a homogeneous Ni complex catalyst (NiL<sub>2</sub>-2L1) and morpholine.**

The one possible reason why the heterogeneous catalyst (Ni-L1@MCM-41) could be utilized for the asymmetric 1,4-addition of nitromethane to alkyldiene malonates is its compatibility toward morpholine (Figure 2-4-1). When morpholine was added to the chiral nickel complex Ni-2L1 (prepared from NiI<sub>2</sub> and L1 in MeCN at 85 °C for 3 h) and stirred in toluene-d<sub>8</sub> for 1 h, free L1 was observed. On the other hand, when morpholine was added to Ni-L1@MCM-41 and stirred in toluene-d<sub>8</sub> for 1 h, the resulting filtrate did not contain any L1. Based on this observation, it appears that ligand dissociation of L1 by morpholine does not occur in a significant amount when Ni-L1 is immobilized on MCM-41.

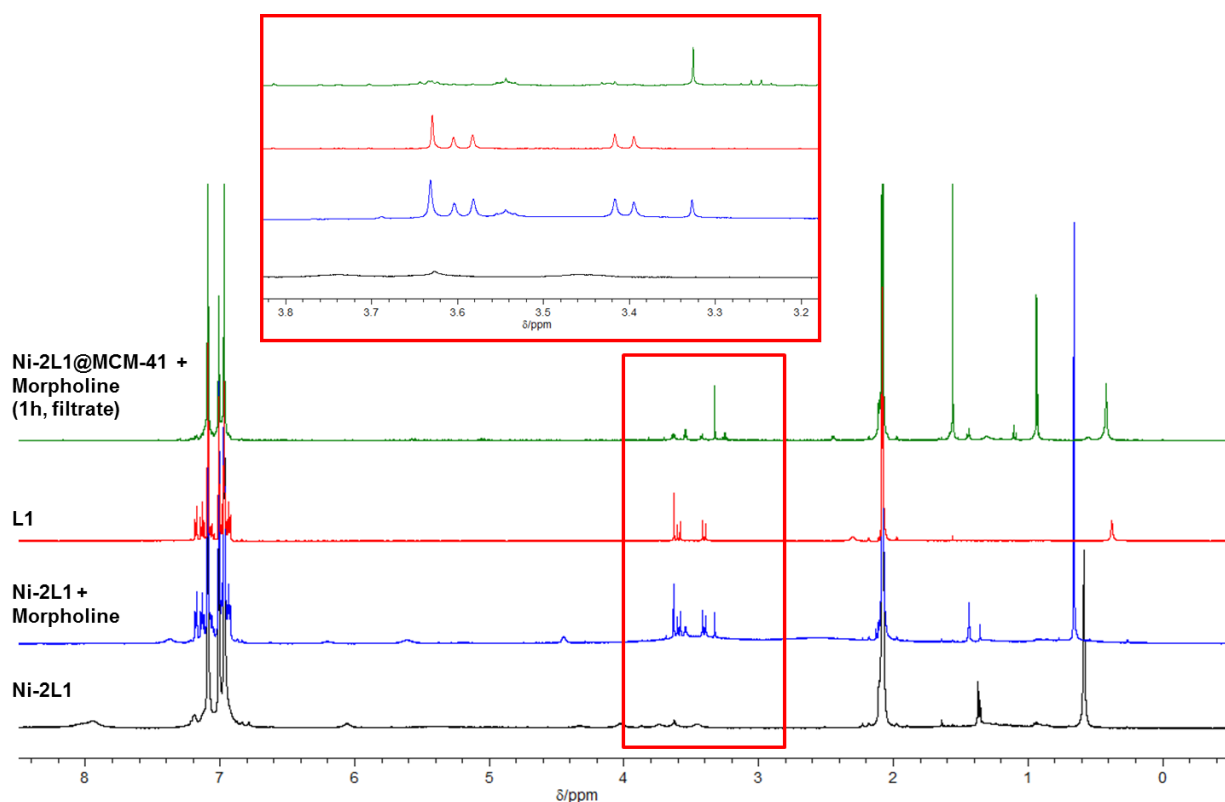
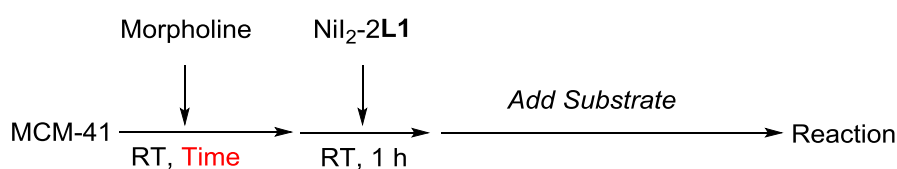
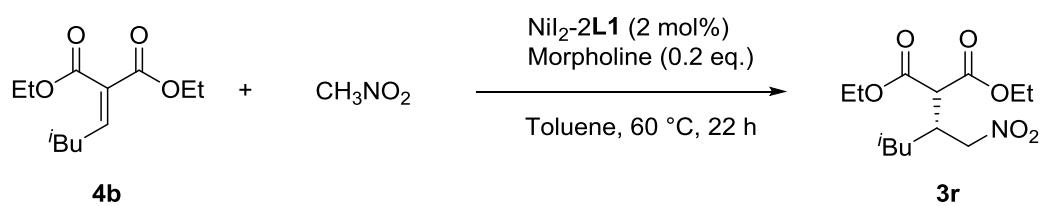


**Figure 2-4-1. <sup>1</sup>H NMR Spectra of the effect of morpholine to Ni-2L1 and Ni-L1@MCM-41 (in toluene-d<sub>8</sub>).**

To clarify the effect of the mesoporous silica for the compatibility with amine, further experiments were conducted. Firstly, morpholine was stirred with MCM-41 in toluene, then, the reaction was conducted by addition of nickel complex solution and substrates to the mixture. When the mixing of morpholine and MCM-41 was performed for 1 hour, the reaction could proceed well. However, as the mixing time diminishing, the yield of the product also decreased, especially 3 minutes mixing provided the product in 37% yield. These results indicated that morpholine rapidly and strongly adsorbed on the support and the adsorbed amine and the Ni complex worked well without decomposition of the complex.

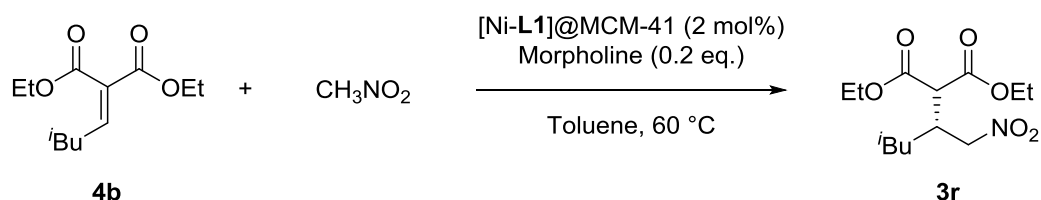
**Table 2-4-2. Experiments to indicate the site separation effect of morpholine and Ni complex**



Entry	Time [min]	Yield [%]
1	60	86
2	15	78
3	3	37

The recovery and reuse of Ni-L1@MCM-41 for the asymmetric addition reaction of nitromethane and alkylidene malonate **4b** was examined (Table 2-4-3). It was found that significant loss in the yield of **3r** was observed, even with the addition of fresh **L1**.

**Table 2-4-3. Recovery and reuse of Ni-L1@MCM-41 for the enantioselective 1,4-addition of nitromethane to alkylidene malonate **4b**<sup>a</sup>**



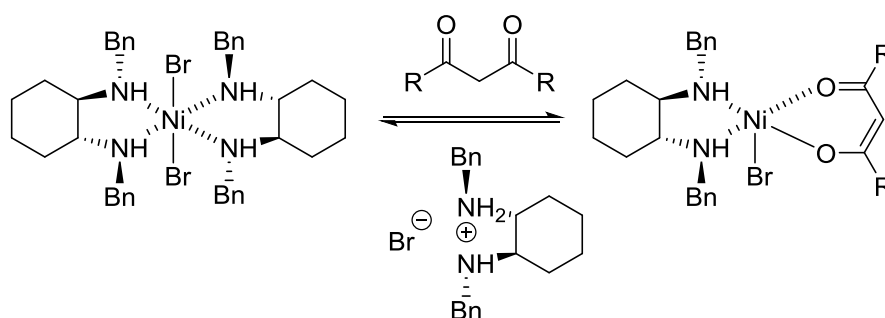
Entry	Run	Ligand (mol%)	Time (h)	Yield (%) <sup>b</sup>	Ee (%) <sup>c</sup>	Leaching (%) <sup>d</sup>
1	1	–	36	79	83	UDL
	2	–	36	12	60	UDL
2	1	–	36	79	83	UDL
	2	2	48	41	80	UDL

<sup>a</sup>Reaction conditions: **4b** (0.25 mmol), nitromethane (0.50 mmol), morpholine (0.05 mmol), and Ni-L1@MCM-41 (2 mol%) in toluene (1.5 mL) at 60 °C. <sup>b</sup>Yields were calculated by GC analysis using tetradecane as an internal standard. <sup>c</sup>Determined by chiral HPLC. <sup>d</sup>Determined by ICP analysis of the recovered reaction filtrate.



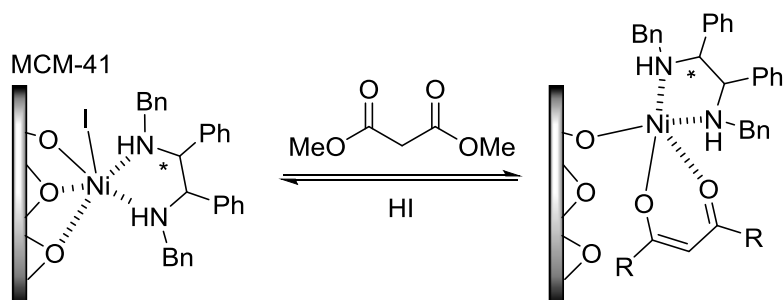
## 2-5 Proposed Mechanism of 1,4-addition Reactions

The prepared heterogeneous catalyst (Ni-L1@MCM-41) was designed based on previous Evans's reports in which enantioselective 1,4-addition of 1,3-dicarbonyl compounds to nitroalkenes catalyzed by nickel(II) diamine complexes was described and the actual active species were proposed (Scheme 2-5-1).<sup>12,13</sup> In their report, an active chiral complex had two chiral diamine ligands and one ligand was exchanged with a bidentate substrate and a liberated chiral ligand acted as a base.



**Scheme 2-5-1. Proposed active species in Evans report**

In the catalysis with Ni-L1@MCM-41, similar events were assumed. When a dimethyl malonate exchanged with oxygen atoms from silica surface, active species for 1,4-addition was generated (Scheme 2-5-2). On the other hand, in the case a dimethyl malonate exchanged with diamine ligand L1, deactivation of the catalyst occurred by dissociation of chiral ligand from Ni center.



**Scheme 2-5-2. Proposed active species in Ni-L1@MCM-41**

As for the asymmetric 1,4-addition of nitromethane to alkylidene malonate (**4**), alkylidene malonate (**4**) coordinated to Ni center to generate chiral environment. An external base, morpholine was required to activate nitromethane, which was reacted with coordinated alkylidene malonate in enantioselective manner.

## 2-6 Utilization of Catalysts for Continuous-flow Reactions

It was described that developed heterogeneous catalyst Ni-L1@MCM-41 has a good catalytic activity under batch conditions. The catalytic active species existed on the surface of MCM-41, which is considered to be suitable for continuous-flow reactions. Therefore, utilization of Ni-L1@MCM-41 for continuous-flow reactions was examined. Considering the reactivity and reusability test, asymmetric 1,4-addition of malonate and nitroalkene bearing *i*Bu moiety which corresponds to pregabalin was investigated with the heterogeneous catalyst under continuous-flow conditions.

As an initial trial, 300 mg of Ni-L1@MCM-41 was packed in a column reactor, toluene solutions of the substrate mixture were fed at the rate of 0.05 mL/min (Figure 2-6-1, red dots ●). The reaction proceeded to provide the desired product **3a** in 74-57% yield during 4-8 hour with good enantioselectivities. Additives packed in the column reactor with catalyst have a potential to improve activity and/or durability of the catalyst. In general, additive materials were mixed with catalysts and the mixture was loaded like method A. Several additives (celite, silica gel, and MCM-41) were packed in the reactor with method A, and the substrate solutions were fed around 8 hours, respectively. Using celite as an additive, there was significant loss of the yield of **3a** (blue triangles ▲). When silica gel was employed, rapid decreasing the yield was observed (yellow triangles ▲). Though MCM-41 was better additive than others, no enhancement of the activity and stability was realized (green triangles ▲ vs. red dots ●). However, a modification of the packing method from method A to method B led to improvement of the stability of the catalytic system (green diamonds ◆) because leached Ni species could be captured by the additional MCM-41. Indeed, after the continuous-flow reaction stopped, recovered additive contained slight amount of Ni species detected by ICP analysis.

On the other hand, I attempted to introduce a pre-column, which put before a column reactor to remove the moisture or other impurities including the solution (Table 2-6-1). As the contents of pre-column, molecular sieves and silica gel were employed and packed in a glass column. A pre-column of MS 4A had an effect on the improvement of activity and stability of continuous-flow system although a pre-column loaded MS 5A and silica gel was not efficient. Based on these results, substrate solutions were prepared in the presence of MS 4A and fed into the column reactor. As a result, the reaction afforded the product in 85% yield but with 66% ee at 8 h since the racemic process could proceed by MS 4A.

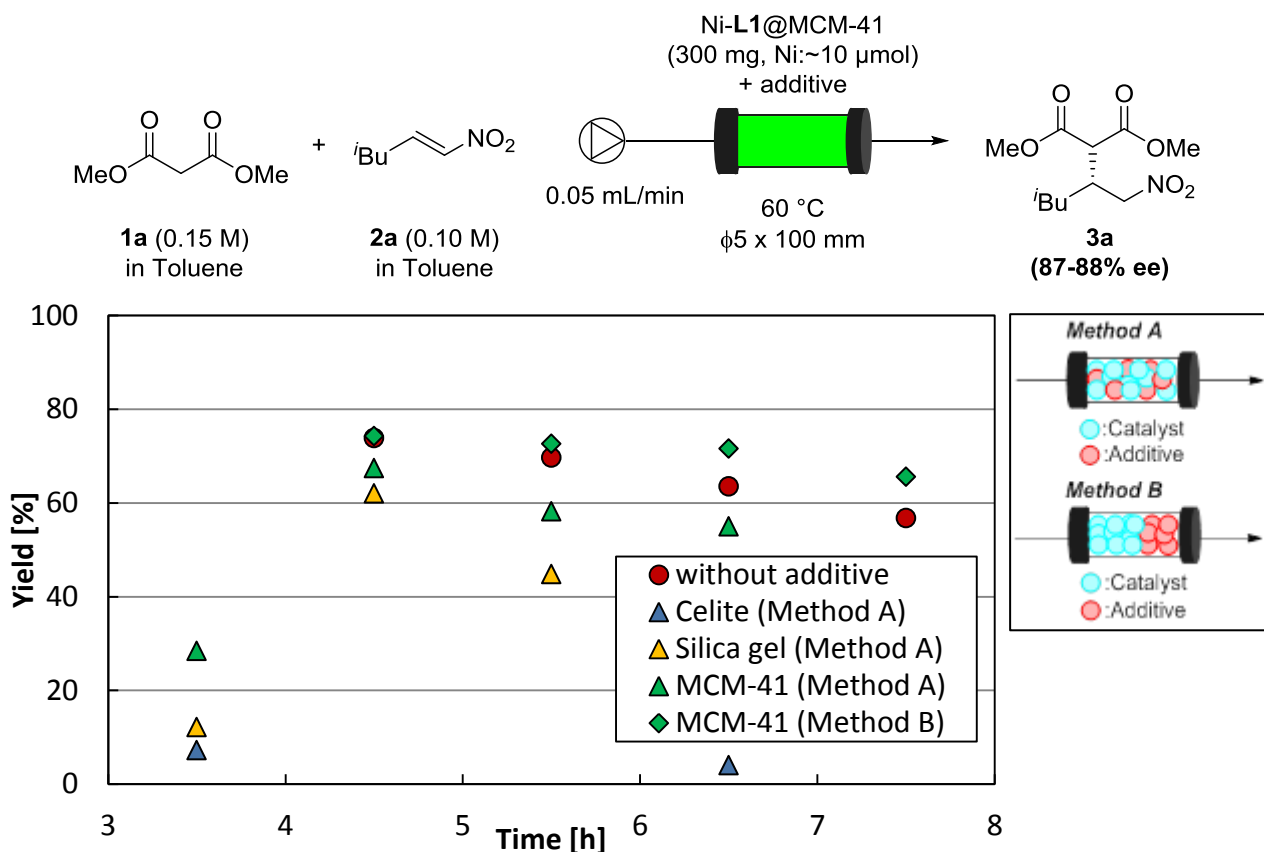
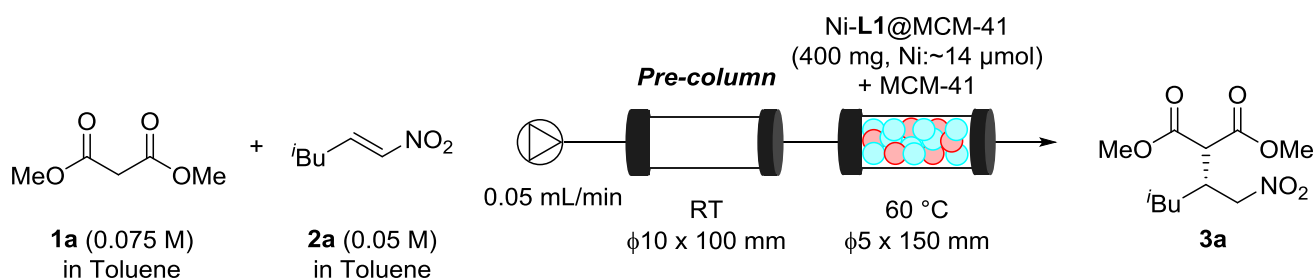


**Figure 2-6-1. Asymmetric 1,4-addition reactions of dimethyl malonate (1a) and nitroalkene (2a) under continuous-flow reaction with several additives.**

**Table 2-6-1. Effect of pre-column for Asymmetric 1,4-addition reactions of 1a and 2a under continuous-flow reaction**



Entry	Pre-column	Time [h]	Yield [%]	Ee [%]
1	MS4A powder	8	87	84
		22	61	84
2	Silica gel	8	ND	-
		22	66	84
3	MS5A powder	8	73	87
		22	44	84

Optimization of additive and pre-column described above facilitated further improvement of continuous-flow system for 1,4-addition of **1a** to **2a**. Introduction of MS 4A pre-column obviously contributed to increasing the yield of **3a** while keeping good enantioselectivity of the product (Figure 2-6-2, green triangles ▲ vs. blue diamonds ◆). Nevertheless, the durability of this system was not enough, rapid decreasing the yield of **3a** was observed at 11 h. Recovery and reuse experiments under batch conditions indicated that the deactivation of the catalyst mainly caused by dissociation of chiral ligand **L1** as described in previous section. Accordingly, 0.2 mol% of **L1** was added to the substrate solution and the mixture was passed through the pre-column and the reactor. Co-feeding of chiral ligand dramatically enhanced the durability of the system, more than 80% yield was maintained for 25 hours (red dots ●), and the maximum TOF reached to 31.3 h<sup>-1</sup> which was higher than TOF in batch reaction (18 h<sup>-1</sup>, 36% yield, 2 h, Ni:1 mol%).

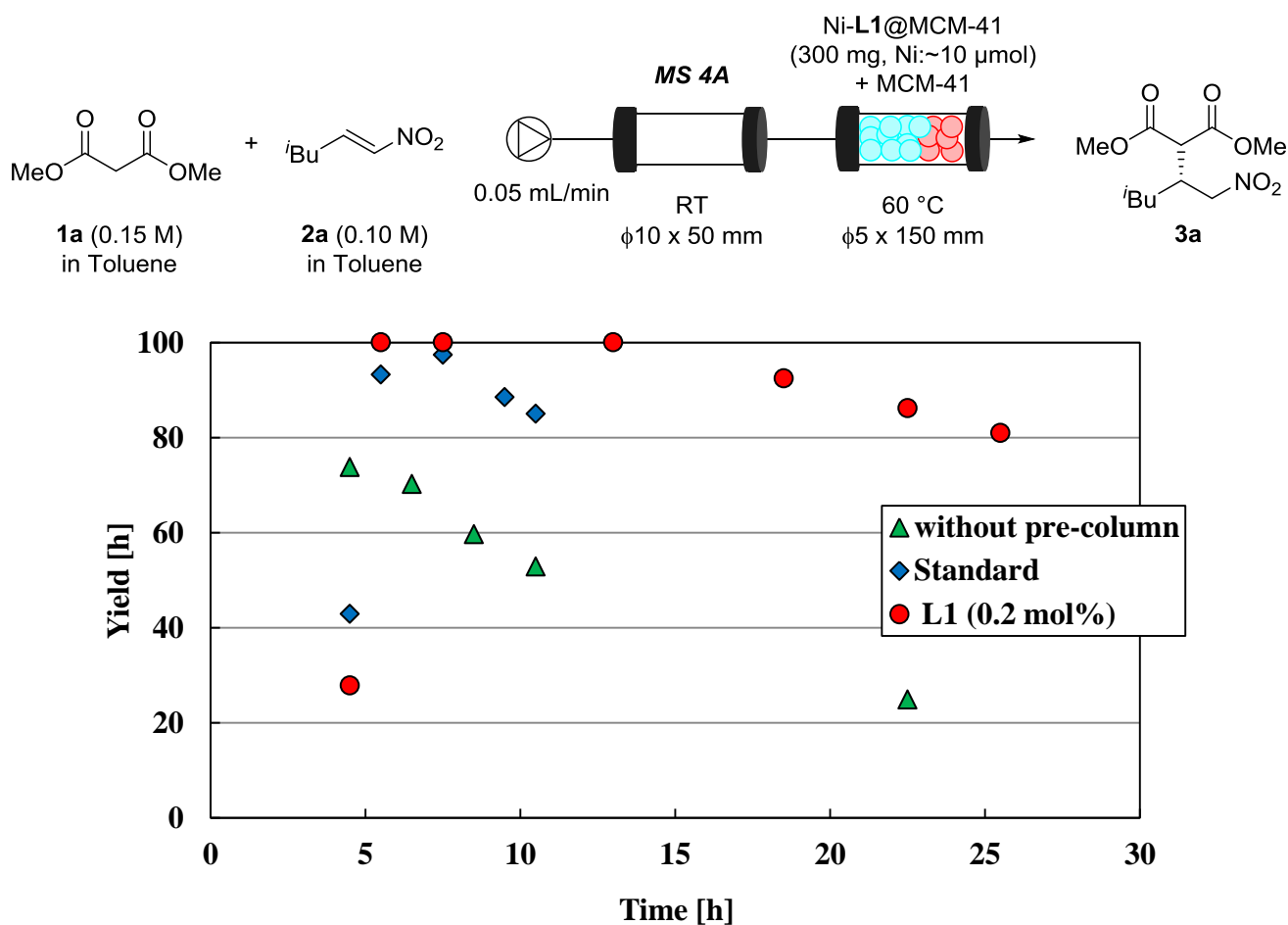
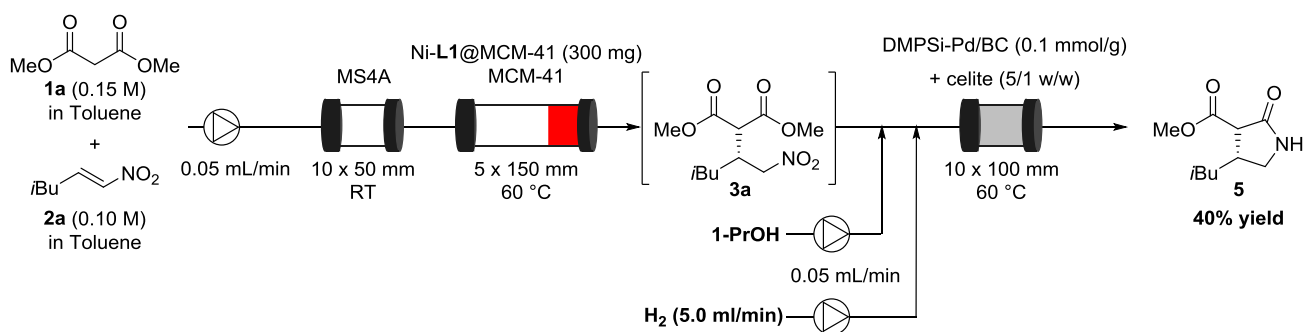


Figure 2-6-2. Further optimization of the conditions for asymmetric 1,4-addition reactions of dimethyl malonate (**1a**) and nitroalkene (**2a**) under continuous-flow reaction

## 2-7 Demonstration of 2-Step Sequential-flow Synthesis of Pregabalin

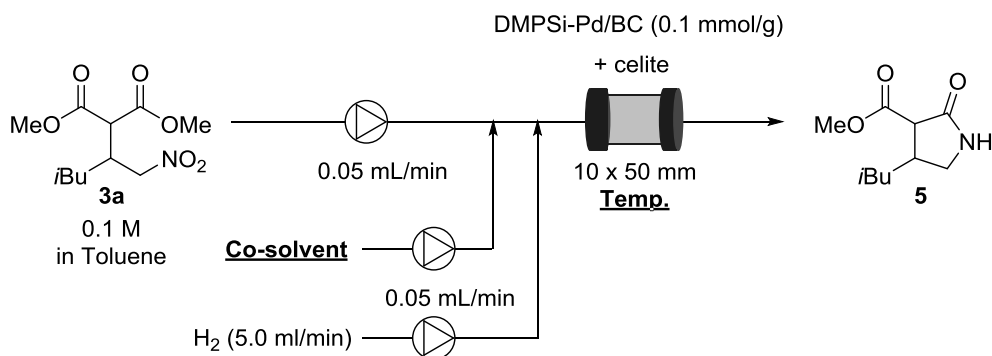
Finally, continuous-flow synthesis of pregabalin was examined by using the developed heterogeneous catalyst in 2-steps sequential flow to demonstrate an application of the catalyst. In previous study,  $\gamma$ -nitro biester **3a** could be transformed to  $\gamma$ -lactam **5** by hydrogenation of nitro group and cyclization catalyzed by a heterogeneous Pd catalyst under continuous-flow condition.<sup>1</sup> Based on this knowledge, an initial trial was performed (Scheme 2-7-1). In first step, enantioselective 1,4-addition of dimethyl malonate **1a** and nitroalkene **2a** utilized by Ni-L1@MCM-41 was employed and the resulting solution eluted from the first step was flowed into the second column reactor with hydrogen gas and 1-propanol as a co-solvent. The second column contained DMPSi-Pd/BC diluted with celite and heated at 60 °C. This 2-step continuous-flow reaction provided the desired product (**5**) in 40% yield in two steps, which indicated that the hydrogenation step was not efficient because the enantioselective 1,4-addition step proceeded and the intermediate (**3a**) was formed in more than 80% yield. Thus, a condition of hydrogenation step was investigated separately from the first step.



**Scheme 2-7-1. Initial attempt for 2-step continuous-flow reaction to synthesis of pregabalin precursor 5**

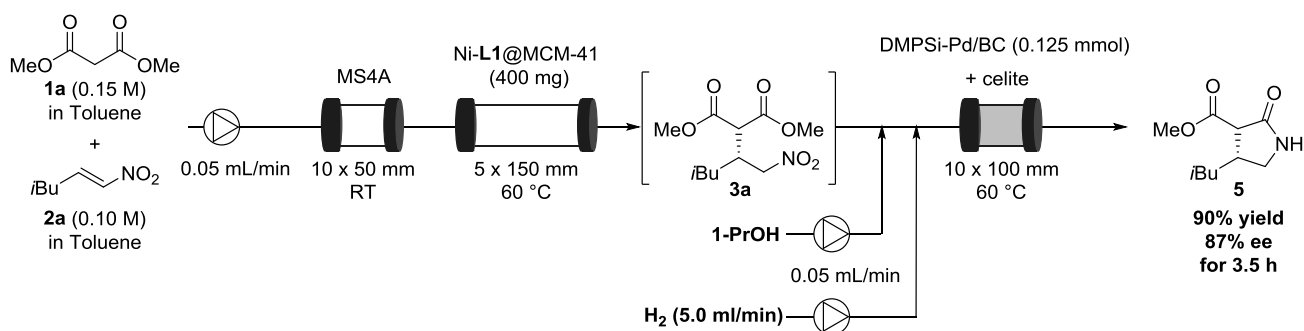
For the examination of the hydrogenation step, a toluene solution of racemic compound **3a** was used and the Pd catalyst (PDMSi-Pd/BC, 0.1 mmol/g) and celite as dilutants were packed in a SUS column ( $\phi$ 10 x 50 mm) (Table 2-7-1). Firstly, 2.5 g of Pd catalyst was loaded and the continuous-flow reaction was carried out with flowing co-solvents, toluene or 1-propanol (entries 1, 2). In these experiments, the desired product was afforded in around 80% yield in spite of full conversion of starting material. It was suggested that much amount of Pd catalyst might adsorbed the product. To solve this problem, catalyst amount was decreased to 1.8 g, the yield of **5** increased to 87% yield (entry 3). In previous study, quantitative transformation from **3a** to **5** could be realized, and further optimization was continued. Finally, 1.25 g of Pd catalyst was enough for excellent yields of the product though a little higher temperature was required (entry 4).

**Table 2-7-1. Investigation of the hydrogenation with Pd catalyst under continuous-flow reaction**



Entry	Co-solvent	Conditions		Results		
		Pd cat [g]	Temp. [°C]	Time [h]	Conv. [%]	Yield [%]
1	Toluene	2.5	60	2-3	ND	4
				4-5	86	77
2	1-PrOH	2.5	60	2-3	full	21
				4-5	full	80
3	1-PrOH	1.8	60	3-4	96	72
				4-5	93	82
				6-7	93	83
				9-9.5	92	87
4	1-PrOH	1.25	80	4-5	ND	ND
				5-6	full	Quant.
				7-8	full	94

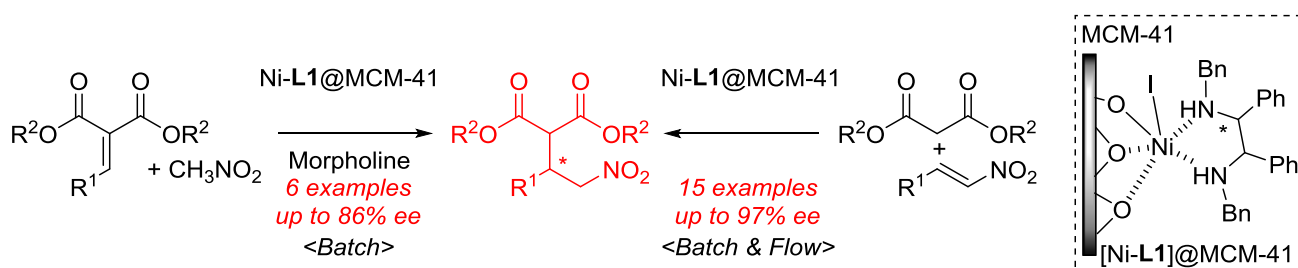
With this optimal condition, 2-step continuous-flow reaction was performed again (Scheme 2-7-2). In addition to the hydrogenation step, continuous-flow condition of asymmetric 1,4-addition step was modified, 400 mg of Ni-L1@MCM-41 was packed in a column reactor without any additives. After stabilization of first step, a subsequent column reactor was connected with feeding a co-solvent and hydrogen gas. As a result, the precursor of pregabalin was obtained in 90% yield in two-steps for 3.5 hours, and the enantioselectivity of **5** was 87% ee, which indicated that the selectivity was maintained during the hydrogenation step. Afforded compound can be converted to pregabalin by acid treatment and neutralization following the literature method.<sup>2</sup>



**Scheme 2-7-2. 2-Step continuous-flow synthesis of pregabalin precursor 5**

## 2-8 Summary

In this chapter, enantioselective 1,4-addition reactions with a developed heterogeneous catalyst have been described. The heterogeneous catalyst Ni-L1@MCM-41 was prepared by just mixing a homogeneous Ni complex and mesoporous silica, MCM-41, which has large surface area and uniform and enough pore size. Immobilized Ni species inside the mesopore had a different structure from the parent homogenous Ni complex revealed by various analyses. Ni-L1@MCM-41 showed superior catalytic activity compared with the homogeneous Ni complex Ni-2L1. Moreover, by immobilization onto the mesoporous silica, Ni species could work even in the presence of an organic base, which led to decomposition of a chiral complex in a homogenous system, and could catalyze enantioselective 1,4-addition of nitromethane to alkylidene malonates to provide the corresponding products in good yields and enantioselectivities. This asymmetric process is the first successful example including homogeneous and heterogeneous catalysis. In addition, a continuous-flow reaction with Ni-L1@MCM-41 was investigated. It was revealed that 1,4-addition of dimethyl malonate to nitroalkene in a continuous-flow manner proceeded well to afford the products in good yields and enantioselectivities by utilizing a MS 4A pre-column before the catalyst packed column reactor. Furthermore, passing the stream eluted from that continuous-flow reaction through a Pd catalyst packed in a column reactor with co-solvent and hydrogen gas, highly efficient asymmetric synthesis of pregabalin under 2-step continuous-flow conditions was established.



Scheme 2-8-1. Summary of chapter 2



## 2-9 References

- (1) H. Ishitani, K. Kanai, Y. Saito, T. Tsubogo, S. Kobayashi, *Eur. J. Org. Chem.* **2017**, 6491–6494.
- (2) H. Y. Bae, C. E. Song, *ACS Catal.* **2015**, *5*, 3613–3619.
- (3) O. Bassas, J. Huuskonen, K. Rissanen, A. M. P. Koskinen, *Eur. J. Org. Chem.* **2009**, 1340–1351.
- (4) T. Okino, Y. Hoashi, T. Furukawa, X. Xu, Y. Takemoto, *J. Am. Chem. Soc.* **2005**, *127*, 119–125.
- (5) M. Terada, H. Ube, Y. Yaguchi, *J. Am. Chem. Soc.* **2006**, *128*, 1454–1455.
- (6) J. Liu, X. Wang, Z. Ge, Q. Sun, T. Cheng, R. Li, *Tetrahedron* **2011**, *67*, 636–640.
- (7) F. Li, Y. S. Jia, M. H. Xu, P. Tian, G. Q. Lin, *Tetrahedron* **2011**, *67*, 10186–10194.
- (8) R. Baran, E. Veverková, A. Škvorcová, R. Šebesta, *Org. Biomol. Chem.* **2013**, *11*, 7705–7711.
- (9) R. S. Tikhvatshin, A. S. Kucherenko, Y. V. Nelyubina, S. G. Zlotin *ACS Catal.* **2017**, *7*, 2981–2989.
- (10) D. Bécart, V. Diemer, A. Salaün, M. Oiarbide, Y. R. Nelli, B. Kauffmann, L. Fischer, C. Palomo, G. Guichard, *J. Am. Chem. Soc.* **2017**, *139*, 12524–12532.
- (11) D. M. Barnes, J. Ji, M. G. Fickes, M. A. Fitzgerald, S. A. King, H. E. Morton, F. A. Plagge, M. Preskill, S. H. Wagaw, S. J. Wittenberger, J. Zhang, *J. Am. Chem. Soc.* **2002**, *124*, 13097–13105.
- (12) D. A. Evans, D. Seidel, *J. Am. Chem. Soc.* **2005**, *127*, 9958–9959.
- (13) D. A. Evans, S. Mito, D. Seidel, *J. Am. Chem. Soc.* **2007**, *129*, 11583–11592.
- (14) M. Studer, H. Blaser, C. Exner, *Adv. Synth. Catal.* **2003**, *345*, 45–65.
- (15) M. Sharma, B. Das, G. V. Karunakar, L. Satyanarayana, K. K. Bania, *J. Phys. Chem. C* **2016**, *120*, 13563–13573.
- (16) J. Li, Y. Ren, C. Qi, H. Jiang, *Chem. Commun.*, **2017**, *53*, 8223–8226.
- (17) R. Jin, K. Liu, D. Xia, Q. Qian, G. Liu, H. Li, *Adv. Synth. Catal.* **2012**, *354*, 3265–3274.
- (18) K. Liu, R. Jin, T. Cheng, X. Xu, F. Gao, G. Liu, H. Li, *Chem. Eur. J.* **2012**, *18*, 15546–15553.

### **Chapter 3. Development of Robust Nickel Immobilized Mesoporous Silica for Asymmetric 1,4-Addition Reactions**

本章については、5年以内に雑誌等で刊行予定のため、非公開。

## Summary

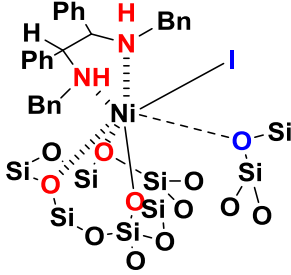
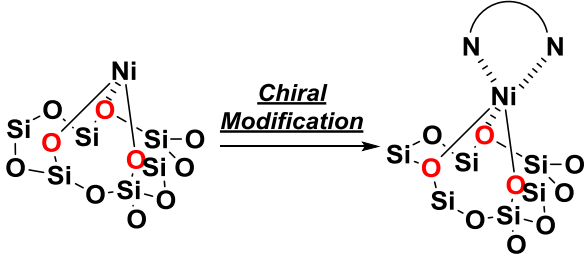
In my Ph. D. thesis, the development of heterogeneous catalysts for asymmetric reactions under continuous-flow conditions was described. In continuous-flow reactions with heterogeneous catalysts, the reactions proceed during adsorption and desorption of substrates to the surface of support materials. Thus, heterogeneous catalysts bearing active sites located on the surface of the support is considered to be suitable for continuous-flow reactions, and immobilization of chiral active sites on the mesoporous silica having high surface area was investigated.

In the first topic, I conducted surface modification of mesoporous silica by a chiral nickel complex, as a result, a novel chiral active species containing I-Ni-OSi bond was constructed within the mesopore of the support. XAFS analysis and other experiments suggested the chemical structure of the chiral active species (Below Table), which had different catalytic activity with reported nickel chiral diamine complexes. In addition, the prepared catalyst Ni-L1@MCM-41 was able to work even in the presence of an organic base, and enantioselective 1,4-addition of nitromethane to alkylidene malonate was developed with Ni-L1@MCM-41 and morpholine as an external base catalyst. This reaction has not been established with other homogeneous and heterogeneous catalysts so far. Continuous-flow reactions with Ni-L1@MCM-41 were efficient and the TOF value reached to 31.3 h<sup>-1</sup> after optimization of a pre-column condition and a packing method of the catalyst. Moreover, this continuous-flow reaction was able to connect with another flow reaction, a hydrogenation reaction of a nitro group by a heterogeneous Pd catalyst, to afford a pregabalin precursor in an enantioselective manner.

In the second topic, the development of a chiral heterogeneous catalyst by chiral modification to nickel species immobilized on the surface of a support was investigated. Ni-immobilized mesoporous silica bearing SiO-Ni-OSi bond (calc.[Ni-L7]@MCM-41) was prepared through surface modification by an achiral Ni complex followed by calcination at high temperature. Modification of a chiral ligand to the Ni species provided chiral catalytic active sites for asymmetric 1,4-addition of dimethyl malonate to nitroalkene. An immobilization method of metal species on the silica material has been developed well; however, in my immobilization method aggregation of Ni was much suppressed compared with Ni-immobilized mesoporous silica prepared by traditional methods. It was found that Ni species were highly dispersed on the surface of mesoporous silica. Especially, calc.[Ni-L7]@MCM-41 showed an advantage as for the stability under continuous-flow reactions, 90 hours continuous operation was achieved by co-feeding of 1 mol% chiral ligand.

In my Ph. D. study, for the sake of the development of efficient chiral heterogeneous catalysts under continuous-flow conditions, two different strategies were utilized; immobilization of a chiral metal complex on the surface and chiral modification to metal species immobilized on the surface. The former catalyst Ni-L1@MCM-41 has a highly catalytic active species, and the latter catalyst has advantage for stability. These methodologies have a potential to apply to other heterogeneous catalysts for asymmetric catalysis under continuous-flow conditions, which may lead to further

development of flow chemistry.

Ni-L1@MCM-41	calc.[Ni-L7]@MCM-41
<p data-bbox="177 461 320 600">Ni Chiral Complex + Mesoporous Silica</p> <p data-bbox="331 461 475 517"><i>Surface Modification</i></p> 	 <p data-bbox="1050 477 1193 533"><i>Chiral Modification</i></p>
<p data-bbox="296 719 671 745">Active Ni silicate (I-Ni-OSi)</p> <p data-bbox="384 757 584 790">TOF = 31.3 h<sup>-1</sup></p> <p data-bbox="384 808 584 842">25 h operation</p>	<p data-bbox="911 719 1334 745">Robust Ni silicate (SiO-Ni-OSi)</p> <p data-bbox="1031 757 1214 790">TOF = 3.3 h<sup>-1</sup></p> <p data-bbox="1023 808 1222 842">90 h operation</p>

## Experimental Section in Chapter 2

### General information

$^1\text{H}$  and  $^{13}\text{C}$  NMR spectra were recorded on JEOL ECX-400, JEOL ECX-500 and a JEOL ECX-600 in  $\text{CDCl}_3$ . Chemical shifts were reported in parts per million (ppm) from tetramethylsilane using the solvent resonance as the internal standard (chloroform:  $\delta$  7.26 ppm) for  $^1\text{H}$  NMR and (deuteriochloroform:  $\delta$  77.0 ppm) for  $^{13}\text{C}$  NMR. IR spectra were measured on a JASCO FT/IR-610 spectrometer. High-resolution mass spectrometry was carried out using a JEOL JMS-T100TD (DART). Preparative thin-layer chromatography (PTLC) was carried out using Wakogel B-5F from Wako Pure Chemical Industries, Ltd. Enantiomeric ratios were determined by chiral HPLC with chiral columns (chiralpak AD-H and OD-H) with hexane and  $^i\text{PrOH}$  as solvents. Inductively Coupled Plasma (ICP) analysis was performed on a Shimadzu ICPS-7510. Nitrogen absorption-desorption isotherm was recorded on a BELSORP-mini Microtrac Bell. X-ray absorption fine structure spectroscopy (XAFS) spectra were obtained from the BL5S1 at the Aichi Synchrotron Radiation Center, Aichi Science & Technology Foundation. STEM/EDS images were obtained using a JEOL JEM-2100F instrument operated at 200 kV. All STEM specimens were prepared by placing a drop of the solution on carbon-coated copper grids and allowed to dry in air (without staining). Calcination under air condition was performed with muffle furnace (KDF S80, As One Co. Ltd.). The XRD patterns were recorded on a Rigaku Miniflex diffractometer.

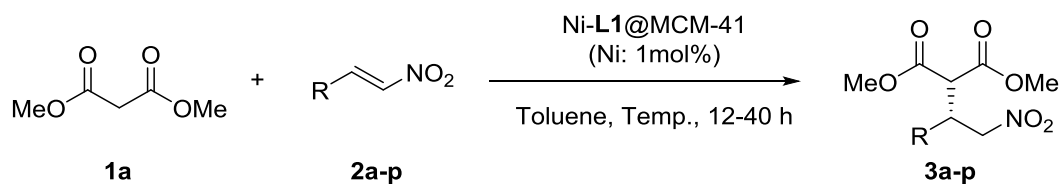
### Reagent

Unless stated otherwise, commercial reagents were used as received. Nitroalkene (**2**) and alkylidene malonate (**4**) used in this study were prepared according to known literature procedures. MCM-41 were prepared according to the literature.<sup>1</sup>

### General procedure of chiral nickel diamine complex immobilized on mesoporous silica (Table 2-2-1, Table 2-2-3)

In a sealed 10 mL one-necked tube, nickel salt (0.005 mmol) and chiral diamine (0.011 mmol) were stirred in MeCN (2 mL) at 85 °C for 3 h. Next, the silica support material, which was used after drying at 100 °C for 1 h under reduced pressure, was added (100 mg) and stirred for 1 h. After filtration of the heterogeneous material, which was washed with DCM and dried under reduced pressure, the catalyst loading was determined by ICP analysis.

**General procedure of enantioselective 1,4-addition reactions of dimethyl malonate (1) to nitroalkenes (2) under batch conditions**



In a 2-necked tube, freshly prepared Ni-L1@MCM-41 (50 mg, 1 mol%), dimethyl malonate (**1a**) (40  $\mu$ L, 0.35 mmol), nitroalkene **2a** (32.3 mg, 0.25 mmol), and toluene (1.5 mL) was stirred for 12 h at 60  $^{\circ}$ C. Next, the reaction mixture was quenched by filtration to separate Ni-L1@MCM-41 from the crude reaction mixture, and was then concentrated *in vacuo*. The resulting organic residue was purified by preparative TLC (1:7 EtOAc:*n*-hexane) to afford **3a** (0.0581 g, 0.223 mmol, 89%, 90% ee) as colorless oil.

**(R)-Dimethyl 2-(4-methyl-1-nitropentan-2-yl)malonate (3a).**<sup>2</sup>  $^1\text{H}$  NMR (500 MHz,  $\text{CDCl}_3$ )  $\delta$  4.71 (1H, dd,  $J = 5.1, 13.0$  Hz), 4.52 (1H, dd,  $J = 6.2, 13.0$  Hz), 3.77 (6H, s), 3.67 (1H, d,  $J = 5.6$  Hz), 2.98–2.95 (1H, m), 1.68–1.62 (1H, m), 1.36–1.28 (2H, m), 0.93 (3H, d,  $J = 5.1$  Hz), 0.92 (3H, d,  $J = 4.5$  Hz);  $^{13}\text{C}$  NMR (125 MHz,  $\text{CDCl}_3$ )  $\delta$  168.3, 168.1, 76.6, 52.7, 52.6, 52.2, 38.8, 34.8, 25.0, 22.3, 22.0. Enantiomeric excess was determined by HPLC analysis with a Chiralpak AD-H column (98:2 hexane:ethanol, 1.0 mL/min, 220 nm); minor enantiomer,  $t_{\text{R}} = 10.6$  min; major enantiomer,  $t_{\text{R}} = 12.0$  min.

**(R)-Dimethyl 2-(1-nitropentan-2-yl)malonate (3b).**<sup>2</sup> Following the above general procedure with **1a** (40  $\mu$ L, 0.35 mmol) and **2b** (0.0288 g, 0.25 mmol) at 60  $^{\circ}$ C for 20 h. The crude reaction mixture was purified by preparative TLC (1:7 EtOAc:*n*-hexane) to afford **3b** (0.0544 g, 0.220 mmol, 88%, 89% ee).  $^1\text{H}$  NMR (500 MHz,  $\text{CDCl}_3$ )  $\delta$  4.71 (1H, dd,  $J = 5.1, 13.1$  Hz), 4.54 (1H, dd,  $J = 6.8, 13.1$  Hz), 3.77 (6H, s), 3.67 (1H, d,  $J = 6.2$  Hz), 2.93–2.90 (1H, m), 1.47–1.37 (4H, m), 0.93 (3H, t,  $J = 6.8$  Hz);  $^{13}\text{C}$  NMR (125 MHz,  $\text{CDCl}_3$ )  $\delta$  168.6, 168.4, 77.5, 53.1, 52.9, 52.5, 36.9, 32.3, 20.0, 13.9. Enantiomeric excess was determined by HPLC analysis with a Chiralcel OD-H column (40:1 hexane:isopropanol, 1.0 mL/min, 210 nm); major enantiomer  $t_{\text{R}} = 11.6$  min, minor enantiomer  $t_{\text{R}} = 24.3$  min.

**(R)-Dimethyl 2-(1-nitrononan-2-yl)malonate (3c).** Following the above general procedure with **1a** (40  $\mu$ L, 0.35 mmol) and **2c** (0.0481 g, 0.25 mmol) at 60  $^{\circ}$ C for 40 h. The crude reaction mixture was purified by preparative TLC (1:7 EtOAc:*n*-hexane) to afford **3c** (0.0501 g, 0.165 mmol, 66%, 87% ee).  $^1\text{H}$  NMR (500 MHz,  $\text{CDCl}_3$ )  $\delta$  4.70 (1H, dd,  $J = 5.1, 13.1$  Hz), 4.53 (1H, dd,  $J = 6.8, 13.1$  Hz), 3.76 (6H, s), 3.67 (1H, d,  $J = 5.7$  Hz), 2.91–2.88 (1H, m), 1.48–1.26 (12H, m), 0.88 (3H, t,  $J = 7.4$  Hz);  $^{13}\text{C}$  NMR (125 MHz,  $\text{CDCl}_3$ )  $\delta$  168.6, 168.4, 77.5, 53.1, 53.0, 52.5, 37.2, 31.9, 30.2, 29.4, 29.2, 26.8, 22.8, 14.3. HRMS(ESI):  $m/z$  calcd for  $\text{C}_{14}\text{H}_{26}\text{NO}_6$  [ $\text{M}+\text{H}^+$ ]: 304.17601. Found: 304.17592.

Enantiomeric excess was determined by HPLC analysis with a Chiralpak AD-H column (98:2 hexane:ethanol, 1.0 mL/min, 220 nm); minor enantiomer  $t_R$  = 15.2 min, major enantiomer  $t_R$  = 19.4 min.

**(R)-Dimethyl 2-(1-nitro-4-phenylbutan-2-yl)malonate (3d).**<sup>2</sup> Following the above general procedure with **1a** (40  $\mu$ L, 0.35 mmol) and **2d** (0.0443 g, 0.25 mmol) at 60 °C for 20 h. The crude reaction mixture was purified by preparative TLC (1:7 EtOAc:*n*-hexane) to afford **3d** (0.0736 g, 0.238 mmol, 95%, 89% ee). <sup>1</sup>H NMR (500 MHz, CDCl<sub>3</sub>)  $\delta$  7.30–7.14 (5H, m), 4.73 (1H, dd,  $J$  = 5.1, 13.1 Hz), 4.56 (1H, dd,  $J$  = 6.8, 13.1 Hz), 3.78–3.70 (6H + 1H, s + d,  $J$  = 5.8 Hz), 2.96–2.92 (1H, m), 2.71–2.68 (2H, m), 1.82–1.77 (2H, m); <sup>13</sup>C NMR (125 MHz, CDCl<sub>3</sub>)  $\delta$  168.1, 168.0, 140.2, 128.6, 128.2, 126.3, 76.3, 52.8, 52.7, 52.2, 36.5, 32.8, 31.7. Enantiomeric excess was determined by HPLC analysis with a Chiralpak AD-H column (9:1 hexanes:isopropanol, 0.7 mL/min, 220 nm); major enantiomer  $t_R$  = 11.2 min, minor enantiomer  $t_R$  = 12.7 min.

**(R)-Dimethyl 2-(1-cyclohexyl-2-nitroethyl)malonate (3e).**<sup>2</sup> Following the above general procedure with **1a** (40  $\mu$ L, 0.35 mmol) and **2e** (0.0388 g, 0.25 mmol) at 60 °C for 40 h. The crude reaction mixture was purified by preparative TLC (1:7 EtOAc:*n*-hexane) to afford **3e** (0.0554 g, 0.193 mmol, 77%, 89% ee). <sup>1</sup>H NMR (500 MHz, CDCl<sub>3</sub>)  $\delta$  4.72 (1H, dd,  $J$  = 4.5, 14.7 Hz), 4.62 (1H, dd,  $J$  = 6.8, 14.7 Hz), 3.80–3.72 (6H + 1H, m), 2.90–2.87 (1H, m), 1.77–1.66 (5H, m), 1.48–1.42 (1H, m), 1.25–0.95 (5H, m); <sup>13</sup>C NMR (125 MHz, CDCl<sub>3</sub>)  $\delta$  168.9, 168.6, 75.4, 53.0, 52.7, 50.9, 42.1, 39.6, 30.1, 29.7, 26.21, 26.16, 26.0. Enantiomeric excess was determined by HPLC analysis with a Chiralpak AD-H column (98:2 hexane:ethanol, 0.7 mL/min, 220 nm); minor enantiomer  $t_R$  = 20.4 min, major enantiomer  $t_R$  = 24.2 min.

**(R)-Dimethyl 2-(3-ethyl-1-nitropentan-2-yl)malonate (3f).**<sup>3</sup> Following the above general procedure with **1a** (40  $\mu$ L, 0.35 mmol) and **2f** (0.0358 g, 0.25 mmol) at 60 °C for 20 h. The crude reaction mixture was purified by preparative TLC (1:7 EtOAc:*n*-hexane) to afford **3f** (0.0647 g, 0.235 mmol, 94%, 88% ee). <sup>1</sup>H NMR (500 MHz, CDCl<sub>3</sub>)  $\delta$  4.69 (1H, dd,  $J$  = 5.1, 14.1 Hz), 4.56 (1H, dd,  $J$  = 6.3, 14.1 Hz), 3.77 (3H, s), 3.73 (3H, s), 3.67 (1H, d,  $J$  = 5.7 Hz), 3.18 (1H, m), 1.35–1.29 (5H, m), 0.92 (6H, dt,  $J$  = 6.8, 18.1 Hz); <sup>13</sup>C NMR (125 MHz, CDCl<sub>3</sub>)  $\delta$  168.7, 168.6, 75.0, 52.9, 52.7, 51.1, 42.7, 38.3, 22.6, 22.3, 11.8, 11.4. Enantiomeric excess was determined by HPLC analysis with a Chiralcel OD-H column (9:1 hexane:isopropanol, 1.0 mL/min, 220 nm); major enantiomer  $t_R$  = 5.6 min, minor enantiomer  $t_R$  = 8.8 min.

**(S)-Dimethyl 2-(2-nitro-1-phenylethyl)malonate (3g).**<sup>2</sup> Following the above general procedure with **1a** (40  $\mu$ L, 0.35 mmol) and **2g** (0.0373 g, 0.25 mmol) at rt for 20 h. The crude reaction mixture was purified by preparative TLC (1:4 EtOAc:*n*-hexane) to afford **3g** (0.0689 g, 0.245 mmol, 98%, 90% ee). <sup>1</sup>H NMR (500 MHz, CDCl<sub>3</sub>)  $\delta$  7.33–7.22 (5H, m), 4.95–4.85 (2H, m), 4.27–4.22

(1H, m), 3.86 (1H, d,  $J = 9.0$  Hz), 3.75 (3H, s), 3.54 (3H, s);  $^{13}\text{C}$  NMR (125 MHz,  $\text{CDCl}_3$ )  $\delta$  167.7, 167.1, 136.0, 128.9, 128.3, 127.8, 77.3, 54.6, 52.9, 52.7, 42.8. Enantiomeric excess was determined by HPLC analysis with a Chiralcel OD-H column (9:1 hexane:isopropanol, 1.0 mL/min, 220 nm); minor enantiomer  $t_{\text{R}} = 14.6$  min, major enantiomer  $t_{\text{R}} = 22.0$  min.

**(S)-Dimethyl 2-(1-(4-chlorophenyl)-2-nitroethyl)malonate (3h).**<sup>2</sup> Following the above general procedure with **1a** (40  $\mu\text{L}$ , 0.35 mmol) and **2h** (0.0459 g, 0.25 mmol) at rt for 20 h. The crude reaction mixture was purified by preparative TLC (1:4 EtOAc:*n*-hexane) to afford **3h** (0.0657 g, 0.208 mmol, 83%, 88% ee).  $^1\text{H}$  NMR (500 MHz,  $\text{CDCl}_3$ )  $\delta$  7.31–7.29 (2H, m), 7.20–7.18 (2H, m), 4.93–4.82 (2H, m), 4.26–4.21 (1H, m), 3.83 (1H, d,  $J = 9.0$  Hz), 3.75 (3H, s), 3.58 (3H, s);  $^{13}\text{C}$  NMR (125 MHz,  $\text{CDCl}_3$ )  $\delta$  167.5, 166.9, 134.5, 134.2, 129.2, 129.1, 77.1, 54.3, 53.0, 52.8, 42.2. Enantiomeric excess was determined by HPLC analysis with a Chiralcel OD-H column (7:3 hexane:isopropanol, 0.7 mL/min, 220 nm); major enantiomer  $t_{\text{R}} = 12.8$  min, minor enantiomer  $t_{\text{R}} = 15.7$  min.

**(S)-Dimethyl 2-(2-nitro-1-(*p*-tolyl)ethyl)malonate (3i).**<sup>2</sup> Following the above general procedure with **1a** (40  $\mu\text{L}$ , 0.35 mmol) and **2i** (0.0408 g, 0.25 mmol) at rt for 20 h. The crude reaction mixture was purified by preparative TLC (1:4 EtOAc:*n*-hexane) to afford **3i** (0.0679 g, 0.230 mmol, 92%, 91% ee).  $^1\text{H}$  NMR (500 MHz,  $\text{CDCl}_3$ )  $\delta$  7.10 (4H, s), 4.92–4.82 (2H, m), 4.23–4.18 (1H, m), 3.84 (1H, d,  $J = 9.1$  Hz), 3.75 (3H, s), 3.53 (3H, s), 2.32 (3H, s);  $^{13}\text{C}$  NMR (125 MHz,  $\text{CDCl}_3$ )  $\delta$  167.9, 167.2, 138.1, 132.9, 129.7, 127.6, 77.5, 54.7, 52.9, 52.8, 42.5, 21.0. Enantiomeric excess was determined by HPLC analysis with a Chiralpak AD-H column (9:1 hexane:isopropanol, 1.0 mL/min, 220 nm); minor enantiomer  $t_{\text{R}} = 12.5$  min, major enantiomer  $t_{\text{R}} = 18.2$  min.

**(S)-Dimethyl 2-(2-nitro-1-(*o*-tolyl)ethyl)malonate (3j).**<sup>2</sup> Following the above general procedure with **1a** (40  $\mu\text{L}$ , 0.35 mmol) and **2j** (0.0408 g, 0.25 mmol) at 50  $^\circ\text{C}$  for 20 h. The crude reaction mixture was purified by preparative TLC (1:4 EtOAc:*n*-hexane) to afford **3j** (0.0472 g, 0.160 mmol, 64%, 91% ee).  $^1\text{H}$  NMR (500 MHz,  $\text{CDCl}_3$ )  $\delta$  7.26–7.11 (4H, m), 4.93–4.83 (2H, m), 4.60–4.55 (1H, m), 3.84 (1H, d,  $J = 9.0$  Hz), 3.76 (3H, s), 3.53 (3H, s), 2.44 (3H, s);  $^{13}\text{C}$  NMR (125 MHz,  $\text{CDCl}_3$ )  $\delta$  167.9, 167.3, 136.9, 134.4, 131.2, 128.0, 126.5, 125.7, 77.3, 54.4, 53.0, 52.8, 37.7, 19.4. Enantiomeric excess was determined by HPLC analysis with a Chiralpak AD-H column (9:1 hexane:isopropanol, 1.0 mL/min, 220 nm); minor enantiomer  $t_{\text{R}} = 9.5$  min, major enantiomer  $t_{\text{R}} = 22.7$  min.

**(S)-Dimethyl 2-(1-(4-methoxyphenyl)-2-nitroethyl)malonate (3k).**<sup>2</sup> Following the above general procedure with **1a** (40  $\mu\text{L}$ , 0.35 mmol) and **2k** (0.0448 g, 0.25 mmol) at rt for 40 h. The crude reaction mixture was purified by preparative TLC (1:4 EtOAc:*n*-hexane) to afford **3k** (0.0756 g, 0.243 mmol, 97%, 97% ee).  $^1\text{H}$  NMR (500 MHz,  $\text{CDCl}_3$ )  $\delta$  7.14 (2H, d,  $J = 8.5$  Hz), 6.83 (2H, d,  $J$



= 9.0 Hz), 4.91–4.80 (2H, m), 4.22–4.17 (1H, m), 3.83 (1H, d,  $J = 9.0$  Hz), 3.76 (6H, s), 3.56 (3H, s);  $^{13}\text{C}$  NMR (125 MHz,  $\text{CDCl}_3$ )  $\delta$  167.8, 167.2, 159.4, 128.9, 127.8, 114.3, 77.6, 55.1, 54.8, 53.0, 52.8, 42.2. Enantiomeric excess was determined by HPLC analysis with a Chiralcel OD-H column (7:3 hexane:isopropanol, 1.0 mL/min, 220 nm); major enantiomer  $t_{\text{R}} = 11.3$  min, minor enantiomer  $t_{\text{R}} = 13.2$  min.

**(S)-Dimethyl 2-(1-(4-(dimethylamino)phenyl)-2-nitroethyl)malonate (3l).**<sup>4</sup> Following the above general procedure with **1a** (40  $\mu\text{L}$ , 0.35 mmol) and **2l** (0.0481 g, 0.25 mmol) at rt for 40 h. The crude reaction mixture was purified by preparative TLC (9:1  $\text{CH}_2\text{Cl}_2$ :*n*-hexane) to afford **3l** (0.0697 g, 0.215 mmol, 86%, 80% ee).  $^1\text{H}$  NMR (500 MHz,  $\text{CDCl}_3$ )  $\delta$  7.03 (2H, d,  $J = 9.0$  Hz), 6.60 (2H, d,  $J = 8.5$  Hz), 4.86–4.76 (2H, m), 4.13–4.09 (1H, m), 3.80 (1H, d,  $J = 9.0$  Hz), 3.71 (3H, s), 3.54 (3H, s), 2.88 (6H, s);  $^{13}\text{C}$  NMR (125 MHz,  $\text{CDCl}_3$ )  $\delta$  168.0, 167.3, 150.0, 128.4, 112.4, 77.7, 54.9, 52.79, 52.78, 52.65, 42.2, 40.2. Enantiomeric excess was determined by HPLC analysis with a Chiralpak AD-H column (7:3 hexane:isopropanol, 1.0 mL/min, 220 nm); minor enantiomer  $t_{\text{R}} = 10.0$  min, major enantiomer  $t_{\text{R}} = 14.3$  min.

**(S)-Dimethyl 2-(1-(naphthalen-2-yl)-2-nitroethyl)malonate (3m).**<sup>5</sup> Following the above general procedure with **1a** (40  $\mu\text{L}$ , 0.35 mmol) and **2m** (0.0498 g, 0.25 mmol) at rt for 40 h. The crude reaction mixture was purified by preparative TLC (1:4 EtOAc:*n*-hexane) to afford **3m** (0.0828 g, 0.25 mmol, quant., 90% ee).  $^1\text{H}$  NMR (500 MHz,  $\text{CDCl}_3$ )  $\delta$  7.82–7.78 (2H, m), 7.70 (1H, s), 7.49–7.46 (2H, m), 7.35–7.33 (1H, m), 5.00 (2H, d,  $J = 6.8$  Hz), 4.45–4.40 (1H, m), 3.97 (1H, d,  $J = 9.0$  Hz), 3.75 (3H, s), 3.52 (3H, s);  $^{13}\text{C}$  NMR (125 MHz,  $\text{CDCl}_3$ )  $\delta$  167.8, 167.2, 133.5, 133.2, 132.9, 128.9, 127.9, 127.6, 127.3, 126.5, 126.4, 125.1, 77.3, 54.7, 53.0, 52.8, 43.0. Enantiomeric excess was determined by HPLC analysis with a Chiralcel OD-H column (7:3 hexane:isopropanol, 1.0 mL/min, 220 nm); minor enantiomer  $t_{\text{R}} = 14.0$  min, major enantiomer  $t_{\text{R}} = 33.4$  min.

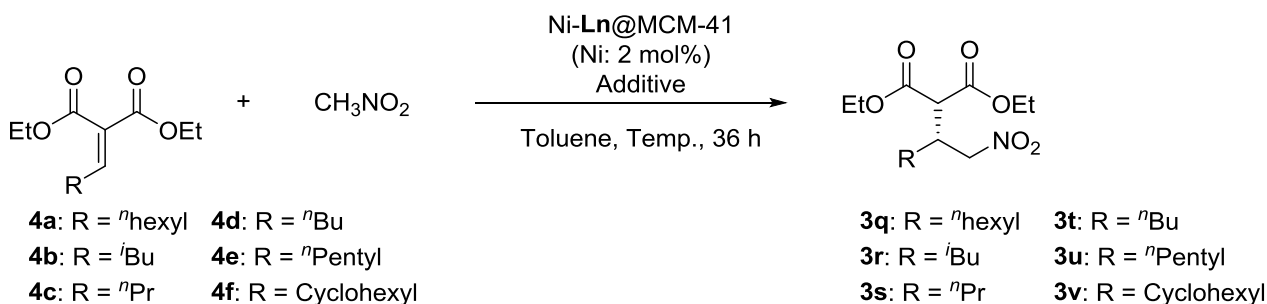
**(R)-Dimethyl 2-(2-nitro-1-(thiophen-2-yl)ethyl)malonate (3n).**<sup>2</sup> Following the above general procedure with **1a** (40  $\mu\text{L}$ , 0.35 mmol) and **2n** (0.0388 g, 0.25 mmol) at rt for 20 h. The crude reaction mixture was purified by preparative TLC (1:4 EtOAc:*n*-hexane) to afford **3n** (0.0704 g, 0.245 mmol, 97%, 90% ee).  $^1\text{H}$  NMR (500 MHz,  $\text{CDCl}_3$ )  $\delta$  7.23 (1H, d,  $J = 5.1$  Hz), 6.95–6.93 (2H, m), 4.94–4.89 (2H, m), 4.57–4.56 (1H, m), 3.92 (1H, d,  $J = 7.9$  Hz), 3.77 (3H, s), 3.67 (3H, s);  $^{13}\text{C}$  NMR (125 MHz,  $\text{CDCl}_3$ )  $\delta$  167.5, 167.1, 138.3, 127.0, 126.7, 125.6, 77.8, 55.2, 53.04, 53.01, 38.3. Enantiomeric excess was determined by HPLC analysis with a Chiralcel OD-H column (4:1 hexane:isopropanol, 1.0 mL/min, 220 nm); minor enantiomer  $t_{\text{R}} = 9.4$  min, major enantiomer  $t_{\text{R}} = 12.1$  min.

**(S)-Dimethyl 2-(1-(1*H*-indol-3-yl)-2-nitroethyl)malonate (3o).**<sup>6</sup> Following the above general procedure with **1a** (40  $\mu\text{L}$ , 0.35 mmol) and **2o** (0.0470 g, 0.25 mmol) at rt for 40 h. The crude

reaction mixture was purified by preparative TLC (9:1 CH<sub>2</sub>Cl<sub>2</sub>:*n*-hexane) to afford **3o** (0.0720 g, 0.225 mmol, 90%, 73% ee). <sup>1</sup>H NMR (500 MHz, CDCl<sub>3</sub>) δ 8.23 (1H, bs), 7.6 (1H, d, *J* = 7.9 Hz), 7.33 (1H, d, *J* = 8.5 Hz), 7.22–7.10 (3H, m), 5.06–4.95 (2H, m), 4.61 (1H, m), 4.11 (1H, d, *J* = 7.9 Hz), 3.71 (3H, s), 3.58 (3H, s); <sup>13</sup>C NMR (125 MHz, CDCl<sub>3</sub>) δ 168.2, 167.8, 136.0, 125.8, 122.8, 122.6, 120.1, 118.2, 111.5, 110.6, 77.1, 54.1, 52.9, 52.8, 34.8. Enantiomeric excess was determined by HPLC analysis with a Chiralcel OD-H column (7:3 hexane:isopropanol, 1.0 mL/min, 220 nm); minor enantiomer *t*<sub>R</sub> = 10.0 min, major enantiomer *t*<sub>R</sub> = 11.5 min.

**(*R,E*)-Dimethyl 2-(1-nitro-4-phenylbut-3-en-2-yl)malonate (3p).**<sup>2</sup> Following the above general procedure with **1a** (40 μL 0.35 mmol) and **2p** (0.0438 g, 0.25 mmol) at 50 °C for 40 h. The crude reaction mixture was purified by preparative TLC (1:4 EtOAc:*n*-hexane) to afford **3p** (0.0768 g, 0.25 mmol, quant., 86% ee). <sup>1</sup>H NMR (500 MHz, CDCl<sub>3</sub>) δ 7.35–7.24 (5H, m), 6.59 (1H, d, *J* = 15.3 Hz), 6.10 (1H, dd, *J* = 15.3, 7.9 Hz), 4.77–4.66 (2H, m), 3.79–3.68 (2H, m), 3.77 (3H, s), 3.73 (3H, s); <sup>13</sup>C NMR (125 MHz, CDCl<sub>3</sub>) δ 167.6, 167.5, 135.8, 135.5, 128.6, 128.2, 126.7, 123.2, 76.9, 53.3, 52.89, 52.86, 41.2. Enantiomeric excess was determined by HPLC analysis with a Chiralpak AD-H column (9:1 hexane:isopropanol, 1.0 mL/min, 220 nm); major enantiomer *t*<sub>R</sub> = 12.9 min, minor enantiomer *t*<sub>R</sub> = 15.6 min.

#### General procedure of enantioselective 1,4-addition reactions of nitromethane to alkylidene malonate (**4**) under batch conditions



In a 2-necked tube, freshly prepared Ni-L1@MCM-41 (100 mg, 2 mol%), alkylidene malonate **4b** (57.1 mg, 0.25 mmol), nitromethane (27 μL, 0.50 mmol), morpholine (4.4 mg, 0.050 mmol), and toluene (1.5 mL) was stirred for 36 h at 60 °C. Next, the reaction mixture was quenched by filtration to separate Ni-L1@MCM-41 from the crude reaction mixture, and was then concentrated *in vacuo*. The resulting organic residue was purified by preparative TLC (1:4 EtOAc:*n*-hexane) to afford **3r** (0.0593 g, 0.205 mmol, 82%, 86% ee) as colorless oil.

**(*R*)-Diethyl 2-(4-methyl-1-nitropentan-2-yl)malonate (3r).**<sup>7</sup> <sup>1</sup>H NMR (400 MHz, CDCl<sub>3</sub>) δ 4.68 (1H, dd, *J* = 6.6, 13.1 Hz), 4.51 (1H, dd, *J* = 6.6, 13.1 Hz), 4.16 (4H, m), 3.58 (1H, d, *J* = 5.8 Hz), 2.95–2.90 (1H, m), 1.66–1.59 (1H, m), 1.35–1.20 (8H, m), 0.90 (3H, d, *J* = 6.3 Hz), 0.89 (3H, d, *J* =

6.3 Hz);  $^{13}\text{C}$  NMR (100 MHz,  $\text{CDCl}_3$ )  $\delta$ 168.0, 167.8, 75.6, 61.9, 61.7, 52.6, 38.9, 34.8, 25.1, 22.3, 22.2, 14.01, 13.99; Enantiomeric excess was determined by HPLC analysis with a Chiralpak AD-H column (99:1 hexane:isopropanol, 0.6 mL/min, 220 nm); major enantiomer  $t_{\text{R}}$  = 19.0 min, minor enantiomer  $t_{\text{R}}$  = 22.4 min.

**(R)-Diethyl 2-(1-nitropentan-2-yl)malonate (3q).**<sup>8</sup> Following the above general procedure with **4a** (53.6 mg, 0.25 mmol). The crude reaction mixture was purified by preparative TLC (1:4 EtOAc:*n*-hexane) to afford **3r** (0.0516 g, 0.188 mmol, 75%, 78% ee).  $^1\text{H}$  NMR (400 MHz,  $\text{CDCl}_3$ )  $\delta$  4.68 (1H, dd,  $J$  = 4.8, 13.4 Hz), 4.51 (1H, dd,  $J$  = 13.4, 6.9 Hz), 4.25–4.15 (4H, m), 3.60 (1H, d,  $J$  = 5.8 Hz), 2.91–2.86 (1H, m), 1.46–1.20 (10H, m), 0.91 (3H, t,  $J$  = 6.5 Hz);  $^{13}\text{C}$  NMR (100 MHz,  $\text{CDCl}_3$ )  $\delta$  168.0, 167.8, 75.6, 61.9, 61.8, 52.6, 36.6, 32.1, 19.8, 14.01, 14.00, 13.8; Enantiomeric excess was determined by HPLC analysis with a Chiralcel OD-H column (97:3 hexane:isopropanol, 1.0 mL/min, 220 nm); major enantiomer  $t_{\text{R}}$  = 6.8 min, minor enantiomer  $t_{\text{R}}$  = 10.8 min.

**(R)-Diethyl 2-(1-nitrohexan-2-yl)malonate (3s).**<sup>8</sup> Following the above general procedure with **4c** (57.1 mg, 0.25 mmol). The crude reaction mixture was purified by preparative TLC (1:7 EtOAc:*n*-hexane) to afford **3s** (0.0573 g, 0.198 mmol, 79%, 83% ee).  $^1\text{H}$  NMR (500 MHz,  $\text{CDCl}_3$ )  $\delta$  4.64 (1H, dd,  $J$  = 5.0, 13.1 Hz), 4.47 (1H, dd,  $J$  = 6.8, 13.1 Hz), 4.20–4.14 (4H, m), 3.56 (1H, d,  $J$  = 5.8 Hz), 2.86–2.79 (1H, m), 1.43–1.38 (m, 2H), 1.31–1.18 (10H, m), 0.83 (3H, t,  $J$  = 7.1 Hz);  $^{13}\text{C}$  NMR (125 MHz,  $\text{CDCl}_3$ )  $\delta$  168.0, 167.8, 76.7, 61.9, 61.8, 52.6, 36.9, 29.7, 28.7, 22.4, 14.01, 13.99, 13.8; Enantiomeric excess was determined by HPLC analysis with a Chiralcel OD-H column (98:2 hexane:isopropanol, 1.0 mL/min, 220 nm); major enantiomer  $t_{\text{R}}$  = 7.1 min, minor enantiomer  $t_{\text{R}}$  = 12.1 min.

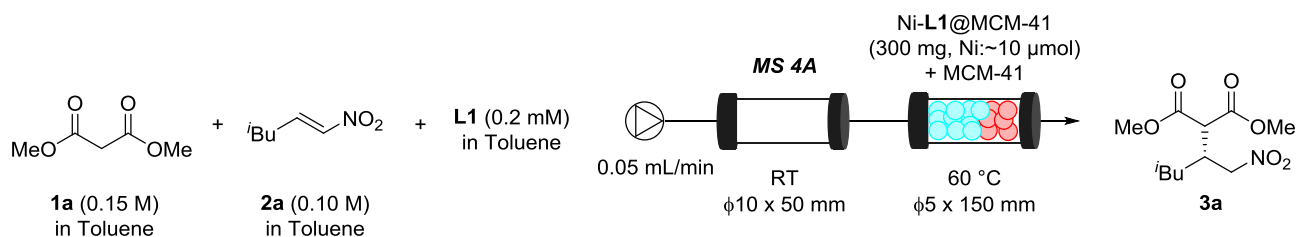
**(R)-Diethyl 2-(1-nitroheptan-2-yl)malonate (3t).**<sup>9</sup> Following the above general procedure with **4d** (60.6 mg, 0.25 mmol). The crude reaction mixture was purified by preparative TLC (1:7 EtOAc:*n*-hexane) to afford **3t** (0.0592 g, 0.195 mmol, 78%, 84% ee).  $^1\text{H}$  NMR (500 MHz,  $\text{CDCl}_3$ )  $\delta$  4.65 (1H, dd,  $J$  = 4.9, 13.3 Hz), 4.48 (1H, dd,  $J$  = 6.8, 13.3 Hz), 4.18–4.11 (4H, m), 3.56 (1H, d,  $J$  = 5.8 Hz), 2.86–2.79 (1H, m), 1.42–1.32 (2H, m), 1.31–1.17 (12H, m), 0.81 (3H, t,  $J$  = 6.8 Hz);  $^{13}\text{C}$  NMR (125 MHz,  $\text{CDCl}_3$ )  $\delta$ 168.0, 167.8, 76.7, 61.9, 61.7, 52.6, 36.9, 31.4, 29.9, 26.2, 22.3, 14.01, 13.99, 13.89; Enantiomeric excess was determined by HPLC analysis with a Chiralcel OD-H column (98:2 hexane:isopropanol, 1.0 mL/min, 220 nm); major enantiomer  $t_{\text{R}}$  = 6.9 min, minor enantiomer  $t_{\text{R}}$  = 11.0 min.

**(R)-Diethyl 2-(1-nitrooctan-2-yl)malonate (3u).**<sup>9</sup> Following the above general procedure with **4e** (64.1 mg, 0.25 mmol). The crude reaction mixture was purified by preparative TLC (1:7 EtOAc:*n*-hexane) to afford **3u** (0.0635 g, 0.200 mmol, 80%, 83% ee).  $^1\text{H}$  NMR (400 MHz,  $\text{CDCl}_3$ )  $\delta$  4.69 (1H, dd,  $J$  = 4.9, 13.3), 4.52 (1H, dd,  $J$  = 6.9, 13.3), 4.25–4.14 (4H, m), 3.61 (1H, d,  $J$  = 6.1

Hz), 2.89–2.85 (1H, m), 1.46–1.39 (2H, m), 1.35–1.20 (14H, m), 0.85 (3H, t,  $J = 6.3$  Hz);  $^{13}\text{C}$  NMR (100 MHz,  $\text{CDCl}_3$ )  $\delta$  168.0, 167.8, 75.6, 61.9, 61.8, 52.6, 36.9, 31.5, 30.0, 28.9, 26.5, 22.5, 14.02, 14.01; Enantiomeric excess was determined by HPLC analysis with a Chiralcel OD-H column (97:3 hexane:isopropanol, 1.0 mL/min, 220 nm); major enantiomer  $t_{\text{R}} = 5.5$  min, minor enantiomer  $t_{\text{R}} = 8.0$  min.

**(R)-Diethyl 2-(1-cyclohexyl-2-nitroethyl)malonate (3v).**<sup>8</sup> Following the above general procedure with **4f** (63.6 mg, 0.25 mmol). The crude reaction mixture was purified by preparative TLC (1:4 EtOAc:*n*-hexane) to afford **3v** (0.0293 g, 0.093 mmol, 37%, 79% ee).  $^1\text{H}$  NMR (400 MHz,  $\text{CDCl}_3$ )  $\delta$  4.70 (1H, dd,  $J = 4.4, 14.3$  Hz), 4.59 (1H, dd,  $J = 6.6, 14.3$  Hz), 4.24–4.13 (4H, m), 3.70 (1H, d,  $J = 4.9$  Hz), 2.89–2.85 (1H, m), 1.75–1.65 (5H, m), 1.44–1.41 (1H, m), 1.31–0.93 (11H, m);  $^{13}\text{C}$  NMR (100 MHz,  $\text{CDCl}_3$ )  $\delta$  168.6, 168.2, 75.5, 62.0, 61.7, 51.4, 42.0, 39.6, 30.2, 29.7, 26.21, 26.17, 26.0, 13.9; Enantiomeric excess was determined by HPLC analysis with a Chiralcel OD-H column (98:2 hexane:isopropanol, 1.0 mL/min, 220 nm); major enantiomer  $t_{\text{R}} = 7.2$  min, minor enantiomer  $t_{\text{R}} = 15.5$  min.

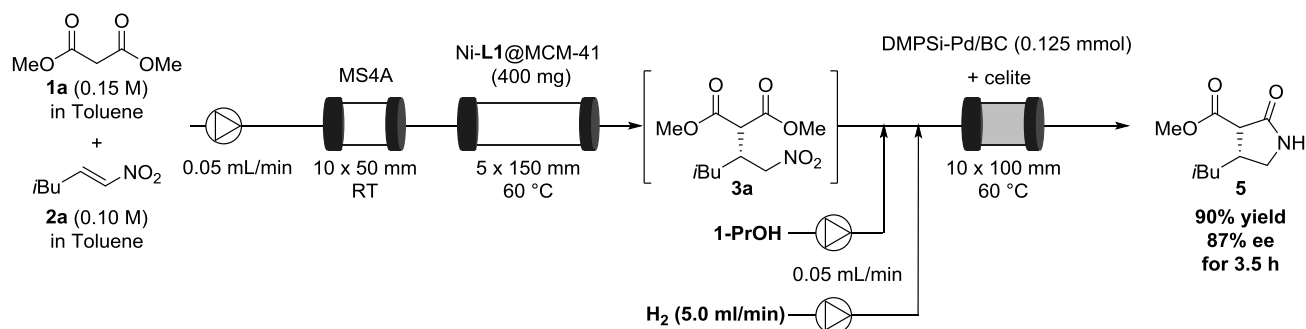
### Procedure of single flow reaction of enantioselective 1,4-addition of malonate (**1a**) to nitroalkene (**2a**) with co-feeding of chiral ligand L1 (Figure 2-5-2)



The continuous-flow reaction of enantioselective 1,4-addition of malonate (**1a**) to nitroalkene (**2a**) was conducted with the set-up illustrated above Scheme. SUS Columns with column ends equipped with filters, HPLC pumps (SHIMADZU LC 20AT), and a column oven (SHIMADZU LC CTO-20AC) were used, and PETF tubes ( $\phi$  0.8 mm) were used to connect the HPLC pumps and columns. The pre-column ( $\phi$  10 x 50 mm) was packed with MS 4A (2 g, Sigma-Aldrich), catalyst column ( $\phi$  5 x 150 mm) was packed with Ni-L1@MCM-41 (300 mg, Ni: 0.039 mmol/g) and MCM-41 (375 mg).

A reaction mixture consisting of **1a** (0.15 M, toluene), **2a** (0.10 M, toluene), and **L1** (0.2 mM, toluene) was flowed into the pre-column and catalyst column (60 °C) at a rate of 0.05 mL/min. The resulting solution was collected for 1 h at appropriate time and 2 mL of collected solution was taken and the solvents were removed under reduced pressure. The crude residue was analyzed by  $^1\text{H}$ -NMR using 1,3,5-trimethylbenzene as an internal standard.

### Procedure of 2-step flow synthesis of pregabalin precursor (**5**) (Scheme 2-6-2)



The two-step continuous flow synthesis of (–)-Pregabalin precursor **5** was conducted with the set-up illustrated above Scheme. SUS Columns with column ends equipped with filters, HPLC pumps (SHIMADZU LC 20AT x 2), and a column oven (SHIMADZU LC CTO-20AC) were used, and PETF tubes ( $\phi$  0.8 mm) were used to connect the HPLC pumps and columns. The pre-column ( $\phi$  10 x 50 mm) was packed with MS 4A (2 g, Sigma-Aldrich), column **A** ( $\phi$  5 x 150 mm) was packed with Ni-L1@MCM-41 (380 mg, Ni: 0.039 mmol/g), and column **B** ( $\phi$  10 x 50 mm) was packed with a mixture of DMPSi-Pd/BC (1.25 g, Pd: 0.1 mmol/g) and Celite 545 (1.25 g, Kokusan Chemical Co.).

A reaction mixture consisting of **1a** (0.15 M, toluene) and **2a** (0.10 M, toluene) was flowed into the pre-column, column **A** (60 °C), and column **B** (80 °C) at a rate of 0.05 mL/min. Concurrently, 1-propanol (0.05 mL/min) and hydrogen gas (5 mL/min) was introduced into column **B** using a Y-shaped connector. The resulting solution was collected for 3.5 h and the solvents were removed under reduced pressure. The crude residue was purified by column chromatography to afford **5** (0.1859 g, 0.933 mmol, 89%, 87% ee)

(**4R**)-Methyl 4-isobutyl-2-oxopyrrolidine-3-carboxylate (**5**).<sup>10</sup> <sup>1</sup>H NMR (500 MHz, CDCl<sub>3</sub>)  $\delta$  6.57 (1H, s), 3.78 (3H, s), 3.56–3.51 (1H, m), 3.06 (1H, d,  $J$  = 8.6 Hz), 2.97–2.90 (2H, m), 1.56–1.48 (1H, m), 1.43–1.31 (2H, m), 0.93 (3H, d,  $J$  = 7.0 Hz), 0.91 (3H, d,  $J$  = 7.0 Hz); <sup>13</sup>C NMR (125 MHz, CDCl<sub>3</sub>)  $\delta$  173.2, 170.3, 54.5, 52.7, 46.6, 43.2, 37.3, 25.9, 22.50, 22.48. Enantiomeric excess was determined by HPLC analysis with a Chiralcel OD-H column (90:10 hexane:isopropanol, 0.7 mL/min, 210 nm); major enantiomer  $t_R$  = 23.4 min, minor enantiomer  $t_R$  = 25.6 min.

## References of Experimental Section in Chapter 2

- (1) a) T. Abe, Y. Tachibana, T. Uematsu, M. Iwamoto, *J. Chem. Soc., Chem. Commun.*, **1995**, 1617-1618; b) M. Iwamoto, T. Abe, Y. Tachibana, *J. Mol. Catal. A; Chemical*, **2000**, *155*, 143-153.
- (2) D. Bécart, V. Diemer, A. Salaün, M. Oiarbide, Y. R. Nelli, B. Kauffmann, L. Fischer, C. Palomo, G. Guichard, *J. Am. Chem. Soc.* **2017**, *139*, 12524.
- (3) P. G. Garcia, A. Zagdoun, C. Copéret, A. Lesage, U. Díaza, A. Corma, *Chem. Sci.* **2013**, *4*, 2006.
- (4) L. Yang, L. Zhao, Z. Zhou, C. He, H. Sun, C. Duan, *Dalton Trans.* **2017**, *46*, 4086.
- (5) K. G. Lewis, S. K. Ghosh, N. Bhuvanesh, J. A. Gladysz, *ACS Cent. Sci.* **2015**, *1*, 50.
- (6) M. Baron, E. Métaý, M. Lemaire, F. Popowycz, *J. Org. Chem.* **2012**, *77*, 3598.
- (7) D. A. Evans, S. Mito, D. Seidel, *J. Am. Chem. Soc.* **2007**, *129*, 11583.
- (8) J. Liu, X. Wang, Z. Ge, Q. Sun, T. Cheng, R. Li, *Tetrahedron* **2011**, *67*, 636.
- (9) M. Lee, L. Zhang, Y. Park, H. Park, *Tetrahedron* **2012**, *68*, 1452.
- (10) H. Y. Bae, C. E. Song, *ACS Catal.* **2015**, *5*, 3613.

### **Experimental Section in Chapter 3**

本章については、5年以内に雑誌等で刊行予定のため、非公開。